UNIVERSIDADE DE SÃO PAULO
CENTRO DE ENERGIA NUCLEAR NA AGRICULTURA

GABRIEL GUSTAVO TAVARES NUNES MONTEIRO

Agroforestry systems as an alternative for the restoration of the biological potential of Amazonian soils

Piracicaba, SP
2025

GABRIEL GUSTAVO TAVARES NUNES MONTEIRO

Agroforestry systems as an alternative for the restoration of the biological potential of Amazonian soils

Revised version according Resolution CoPGr6018 from 2011

Dissertation presented to the Center for Nuclear Energy in Agriculture of the University of São Paulo as a requirement for the Master Degree in Sciences

Concentration Area: Biology in Agriculture and Environment

Advisor: Profª. Dra. Tsai Siu Mui

Piracicaba, SP
2025

Dados Internacionais de Catalogação na Publicação (CIP)

Seção Técnica de Biblioteca - CENA/USP

Monteiro, Gabriel Gustavo Tavares Nunes

Sistemas agroflorestais como alternativa para a restauração do potencial biológico dos solos amazônicos / Agroforestry systems as an alternative for the restoration of the biological potential of Amazonian soils / Gabriel Gustavo Tavares Nunes Monteiro; orientadora Tsai Siu Mui. - - Versão revisada de acordo com a Resolução CoPGr 6018 de 2011. - - Piracicaba, 2025.

83 p.

Dissertação (Mestrado – Programa de Pós-Graduação em Ciências. Área de Concentração: Biologia na Agricultura e no Ambiente) – Centro de Energia Nuclear na Agricultura da Universidade de São Paulo.

1. Carbono orgânico total 2. Ecologia microbiana 3. Florestas tropicais - Amazônia 4. Matéria orgânica do solo 5. Sistemas agroflorestais 6. Uso do solo I. Título

CDU 630*114(811.3)

Elaborada por:

Marilia Ribeiro Garcia Henyei

CRB-8/3631

Resolução CFB Nº 184 de 29 de setembro de 2017

ACKNOWLEDGEMENTS

To life and the universe, who have always guided me through many coincidences and happy accidents. The academic path is often arduous, but doing science is fascinating and gratifying. It's been fun, and I am grateful for everything that happened along the way.

To my family, especially my parents, Núbia and Néliton, and to my dear aunt Nilza and uncle Nato. Your encouragement and love have guided me here, and through this path, I have found true happiness. Thank you so much for your teachings and support, you are my eternal gratitude.

To Professor Tsai, whom I had the pleasure (and the privilege) of having as an advisor. Your research found me before this endeavor and sparked my passion for soil microbiology. At the end, I had the opportunity to be your student and witness all your life and academic wisdom. Thank you for this opportunity and guidance.

To Professor Gerd Gleixner, your research was the seed that sparked the ideas that formed this work, and your teachings certainly made me a better scientist and person. Our paths have crossed without realizing it, and I had the chance to be your exchange student. Thank you for agreeing to collaborate with this research and welcoming me to the Max Planck Institute for Biogeochemistry. It was a unique opportunity to witness biogeochemistry at its peak.

To my previous advisors, Candido Ferreira, Joyce Kelly, Vania Neu, and Acácio Navarrete, thank you for all your teachings and advice. I wouldn't be here without you.

To Yan Cardoso, my best friend who witnessed this journey since it started. From the very first day of university to grad school, you were always by my side, supporting the craziest ideas and listening to frantic rambles about everything. Thank you for your friendship and encouragement.

To Thierry Alexandre Pellegrinetti, Anderson Santos de Freitas, Guilherme Lúcio Martins, Gabriele Rossini, and Izadora Cunha, for your friendship and mentorship. You guys might not have noticed, but your friendship, help, and teachings jointly paved the way for this work.

To Frederik Lange, Jessica Fink, Arina Ivanova, Alice Orne, Chen Huang, Georg Dittman, and Peter Sander, your teachings and friendship were essential parts of my internship.

To the researchers and technicians of the Max Planck Institute for Biogeochemistry, especially to Valerie Schwab-Lavric, Ines Hilke, Kerstin Lohse, Iris Kuhlmann, Savoyane Lambert, and Gundula Redlich. You have guided me from the beginning to the end of my stay at the MPI-BGC, and your work inspires me.

To everyone at the Cell and Molecular Biology Laboratory, especially to Ana, Juan, Jessica, Lara, Luana, Henrique, Solange, Sayuri, and Lucas M., our daily exchanges, your friendship, and experiences were essential for this work. The laboratory has so many exceptional people, even though not mentioned by name, I would like to thank all the technicians, students, interns, and visitors.

To Dr. Rafael Moyses Alves and the Cooperativa Agrícola Mista de Tomé-Açu (CAMTA) and their farmers for the support and opportunity to study the agroforests of Tomé-Açu.

To the National Council for Scientific and Technological Development (CNPq, process nº 167188/2022-4) and São Paulo Research Foundation (FAPESP, process nº 2023/07080-1 and 2024/02443-1) for granting the master's scholarships and international exchange scholarship.

Muito obrigado | Thank you | Danke schön

“Essentially, all life depends upon the soil. There can be no life without soil and no soil without life. They have evolved together”

(Charles E. Kellogg | 1938)

“How can I stand on the ground every day and not feel its power? How can I live my life stepping on this stuff and not wonder at it?”

(William Bryant Logan | 2007)

ABSTRACT

MONTEIRO, G. G. T. N. **Agroforestry systems as an alternative for the restoration of the biological potential of Amazonian soils**. 2025. 83 p. Dissertação (Mestrado em Ciências) – Centro de Energia Nuclear na Agricultura, Universidade de São Paulo, Piracicaba, 2025.

The Amazon is experiencing increasing deforestation and agricultural expansion, leading to biodiversity loss and soil degradation. The removal of plant cover accelerates the depletion of the surface organic layer, resulting in a decline in soil fertility. In response, agroforestry systems (AFS) have been proposed as a sustainable alternative for agricultural production in the region. Here, we established a land-use sequence from a degraded pasture to 7, 35, and 50-year-old AFS, culminating in an undisturbed primary forest in the Eastern Amazon, to evaluate the effects of long-term cocoa AFS in soil health using a composite index based on physicochemical properties, enzymatic activities (β-glucosidase, acid phosphatase, and arylsulfatase), and microbial abundance and diversity (bacteria and fungi). The results showed that 50-year-old AFS exhibited chemical and biological characteristics — such as litter accumulation, and higher levels of nitrogen, phosphorus, and dissolved organic carbon — comparable to those of primary forests. Carbon stocks increased progressively along the AFS chronosequence, peaking at 77.9 Mg C ha^{-1} after 50 years, a 44.8% increase when compared to pastures, although remaining far below the 124.13 Mg C ha^{-1} found in primary forests. Bacterial abundance was higher in pastures than in AFS and primary forests, while fungal abundance was greatest in forested areas. Older AFS promoted increased fungal diversity and reduced bacterial dominance, particularly in deeper soil layers. The soil health index indicated that AFS reached levels similar to primary forests after 35 years, but this similarity was mostly restricted to the top 10 cm of soil. Notably, the biological component of the index in 50-year-old AFS was equivalent to that of primary forests. These findings collectively indicate that agroforests can maintain and gradually enhance critical soil functions to levels similar to primary forests through the accumulation of carbon across the distinct soil layers, especially in the litter. Altogether, the agroforests presented as an alternative for long-term (> 35 years) sustainable cocoa production in the Amazon.

Keywords: Agroforestry systems. Soil organic carbon. Microbial ecology. Soil health.

RESUMO

MONTEIRO, G. G. T. N. **Sistemas agroflorestais como alternativa para a restauração do potencial biológico dos solos Amazônicos**. 2025. 83 p. Dissertação (Mestrado em Ciências) – Centro de Energia Nuclear na Agricultura, Universidade de São Paulo, Piracicaba, 2025.

A Floresta Amazônica tem vivenciado crescente expansão agrícola e aumento do desmatamento, resultando em perdas de biodiversidade e do solo. A remoção da cobertura vegetal acelera o esgotamento da camada orgânica superficial, ocasionando declínio na fertilidade do solo e consequente abando de grandes extensões de terras para regeneração natural. Em resposta, sistemas agroflorestais (SAFs) vêm sendo propostos como uma alternativa sustentável para a produção agrícola na região. Neste estudo, estabelecemos uma sequência de uso da terra, partindo de uma pastagem degradada até SAFs de 7, 35 e 50 anos, culminando em uma floresta primária intocada na Amazônia Oriental, para avaliar os efeitos a longo prazo de SAFs na saúde do solo, através de um índice composto baseado em propriedades físico-químicas, atividades enzimáticas (β-glicosidase, fosfatase ácida e arilsulfatase), abundância e diversidade microbiana (bactérias e fungos). Os resultados mostraram que o SAF de 50 anos apresentou características químicas e biológicas — como acúmulo de serapilheira e níveis mais elevados de nitrogênio, fósforo e carbono orgânico dissolvido — comparáveis às das florestas primárias. Os estoques de carbono aumentaram progressivamente ao longo da cronossequência de SAFs, atingindo 77.9 Mg C ha^{-1} após 50 anos, o que representa um aumento de 44.8% quando comparado com a pastagem, ao mesmo tempo que permanece bem abaixo dos 124.13 Mg C ha^{-1} encontrados nas florestas primárias. A abundância bacteriana foi maior em pastagens do que em SAFs e florestas primárias, enquanto a abundância fúngica foi mais elevada em áreas florestais. SAFs mais antigos promoveram aumento na diversidade fúngica e redução do domínio bacteriano, particularmente em camadas mais profundas do solo. O índice de saúde do solo indicou que os SAFs alcançaram níveis semelhantes aos das florestas primárias após 35 anos, mas essa similaridade se restringiu principalmente aos primeiros 10 cm do solo. Notavelmente, o componente biológico do índice em SAFs de 50 anos foi equivalente ao das florestas primárias. Esses achados indicam, de forma conjunta, que os SAFs conseguem manter e gradualmente aprimorar funções críticas do solo a níveis semelhantes aos das florestas primárias através do acúmulo contínuo de carbono nas diversas camadas do solo, especialmente na serrapilheira. Dessa forma, apresentando uma alternativa para a produção sustentável de cacau em longo prazo (> 35 anos) na Amazônia.

Palavras-chave: Sistemas agroflorestais. Carbono orgânico do solo. Ecologia microbiana. Saúde do solo.

SUMMARY

1. INTRODUCTION 13
1.1. Thesis outline 16
1.1.1. Hypothesis 16
1.1.2. Objectives 16
1.1.3. Specific objectives 16
2. MATERIAL AND METHODS 17
2.1. Study area and site description 17
2.2. Litter and soil sampling 19
2.3. Litter chemical analysis 20
2.4. Soil physical and chemical properties 21
2.5. Litter and soil C and N concentrations and isotopic composition 21
2.8. Litter and soil DNA extraction and purification 23
2.9. Quantitative polymerase chain reaction and amplicon sequencing 24
2.10. Bioinformatics 24
2.11. Soil health index calculation 25
2.12. Data analysis 25
3. RESULTS 27
3.1. Litter and soil chemical composition 27
3.2. C and N stocks and their isotopic signature 30
3.2.1. Litter layer 30
3.2.2. Soils 32
3.2.3. Particulate and mineral-associated soil organic matter fractions 34
3.5. Influence of AFS succession on soil enzyme activity 39
3.6. Bacterial and fungal abundance 41
3.7. Effects of land use succession on litter-associated bacterial and fungal assembly 42
3.8. Effects of land use succession on soil bacterial and fungal assembly 46
3.9. Depth-stratified soil bacterial and fungal indicator taxa across a land-use successional gradient 50
3.10. Soil health index (SHI) scores 51

4. DISCUSSION 54

4.1. AFS progression and recovery of ecosystem functions 54

4.2. Agroforest succession increased microbial activity and abundance in a depth-stratified pattern 56

4.3. AFS exhibit divergent microbial communities as they develop 56

4.4. Soil Health Index as an integrative indicator of succession 60

5. CONCLUSION 61

REFERENCES 62

APPENDICES 73

1. INTRODUCTION

Tropical rainforests are among the world's most complex and biodiverse ecosystems, and the Amazon rainforest is the largest of them (Condit et al., 2002; Slik et al., 2015), harboring vast biodiversity of plants, animals, and microorganisms (Jenkins et al., 2013; Navarrete et al., 2015; Slik et al., 2015). Its sheer size and diversity are mainly driven by the homogenous climate, abundant solar radiation, and high precipitation rates, enabling biomass production of up to 300 Mg ha^{-1}, even under heavy soil nutrient constraints (Davidson et al., 2004; Saatchi et al., 2007; Usinowicz et al., 2017).

Soils across the central Amazon are highly weathered and nutrient-poor, lacking natural nutrient retention capacity (Davidson et al., 2004). Due to the high precipitation rates typical of the humid (sub)tropical areas and low charge density across mineral surfaces, almost all soluble molecules have leached out (Xu et al., 2016). The heavy nutrient constraints have shaped species distribution and driven several evolutionary adaptations to acquire and conserve nutrients (Jordan; Herrera, 1981). For instance, trees are able to develop dense root mats in the soil surface and enhance root-microbe interactions for nutrient solubilization and acquisition (Herrera et al., 1978; Lugli et al., 2021). Nutrients thus mostly accumulate in the aboveground tree biomass, heavily relying on belowground microbial communities for constant decomposition of organic matter and subsequent nutrient cycling (Flores et al., 2020).

To better explore the nutrient reserves of forest biomass, tropical farmers traditionally practice the so-called 'slash-and-burn' method for converting primary and secondary forests to agricultural lands (Marquardt et al., 2019). In the 'slash-and-burn' practice, the plant biomass accumulated after the forest clear-cutting is gathered and burned, and the resulting ashes are incorporated into the soil to increase fertility (D'Oliveira et al., 2011; Marquardt et al., 2019). This process results in the complete or partial loss of the aboveground and belowground carbon stocks in the form of CO2 (Nunes et al., 2022). The loss of the native vegetation cover and greater exposure of the weathered and nutrient-poor soils to the tropical climate results in the rapid loss of soil fertility and land degradation, with subsequent loss of productivity after just a few years of use (Davidson et al., 2012; Laurance et al., 1999; Markewitz et al., 2004; Schaefer et al., 2008). Altogether, this makes the traditional agricultural production systems unsustainable long-term, leading to the abandonment of large, degraded areas for natural regeneration (Villa et al., 2018).

Therefore, appropriate management and the restoration and maintenance of the soil capacity to sustain plants, animals, and humans are essential for sustainable agriculture in the Amazon (Leite et al., 2023). Thus, farmers developed strategies to mimic some of the native forest's essential characteristics to prevent soil degradation, promote carbon and nutrient accumulation in plant biomass, and enable nutrient cycling and organic matter buildup through interactions among plants, soil, and microorganisms.

Figure 1. Representation of the multiple layers in an agroforestry system. Adapted from Elevitch et al. (2018)

Agroforestry is a land use system based on crop diversification, coupling perennial woody trees with crops and/or animals to optimize production per unit of area and enhance integration between components (Atangana et al., 2014; Nair, 2014) (Figure 1). This system relies on the capacity of trees to explore and acquire nutrients from different soil layers, recycling them via litter deposition in a system called nutrient pumping (Isaac and Borden, 2019; Seneviratne et al., 2006). The main benefit of agroforestry systems lies in improving ecosystem resource management through better nutrient use efficiency and cycling, all while supporting sustainable food and crop production over the long term.

Agroforestry systems (AFS) present a promising alternative for restoring degraded areas and sustainable crop production in the tropics in a structure resembling native forests (Cezar et al., 2015; Jose, 2009; Nair, 2013; Young, 2017). When correctly managed, AFS can improve soil properties and provide ecosystem services such as carbon sequestration, decreased nutrient losses, and pest regulation (Celentano et al., 2020; Mohri et al., 2013; Pinho et al., 2012). The increased interaction between the agroforest's different components also provides efficient management of ecosystem resources, effectively enhancing productivity and potentially aiding in the restoration of soil quality and ecosystem resilience (Lorenz; Lal, 2018; Nair, 2014; Nair et al., 2010; Pinho et al., 2012). Therefore, trees in agroforestry systems might contribute significantly to the sustainability of crop production by playing two central roles: nutrient acquisition and soil conservation.

Agroforestry integrates biophysical, environmental, socio-economic, and cultural factors. They can be functionally diverse and economically complex, with various designs and management strategies tailored to each farmer's needs (Atangana et al., 2014). Thus, AFS design and management changes can directly affect the type and quantity of organic carbon transferred in the soil via litterfall and rhizodeposition (Ayres et al., 2009). Through these mechanisms, plants can release thousands of organic molecules into the soil, fueling microbial metabolism and shaping microbial community composition (Gmach et al., 2020). In turn, during its passage through the soil profile, organic molecules can be selectively immobilized by organo-mineral interactions into the surface of minerals or incorporated into microbial biomass and re-released in the form of altered compounds upon cell death (Kaiser; Kalbitz, 2012; Roth et al., 2019). These interactions can shape the carbon distribution in the different fractions of soil organic matter and modulate many soil characteristics (Cotrufo; Lavallee, 2022). Such processes are critical in Amazonian soils due to their low capability for nutrient retention (Laurance et al., 1999; Schaefer et al., 2008).

Currently, the dynamics of aboveground-belowground interactions in tropical agricultural systems and their role in ecosystem stability are poorly understood, thus needing further research on how agroforest systems can shape belowground processes and the soil microbiome through changes in the soil organic matter.

1.1. Thesis outline

1.1.1. Hypothesis

Based on the knowledge that increasing aboveground diversity increases microbial activity and soil carbon storage (Lange et al., 2015), we hypothesize that (*i*) agroforestry systems (AFS) can enhance soil carbon accumulation with time, recovering carbon storage in deeper layers; (*ii*) AFS can modulate multiple soil physicochemical parameters, ultimately resulting in higher microbial abundance and diversity, reaching levels close to those found in native forests; (*iii*) through multidimensional changes, AFS can increase and restore soil health with time.

1.1.2. Objectives

The general goal of this thesis was to investigate whether AFS can enhance soil microbial activity and organic carbon accumulation and whether these changes in soil carbon dynamics are reflected in the composition of bacterial and fungal communities.

1.1.3. Specific objectives

To test our hypothesis and achieve the general aim of this thesis, we structured the research around the following objectives: (*i*) evaluate the effects of the established land use sequence from degraded pastures, to 7-, 35-, 50-year-old AFS and primary forest on the soil physicochemical properties and soil organic matter storage; (*ii*) investigate the effects of the land use gradient in the microbial community composition and diversity through 16S ribosomal RNA (16S rRNA) and Internal Transcribed Spacer (ITS) regions quantitative polymerase chain reaction (qPCR) and amplicon sequencing; (*iii*) explore the capacity of those systems to restore the carbon and microbial dynamics to levels closer to the primary forest through multidimensional analysis.

2. MATERIAL AND METHODS

2.1. Study area and site description

The study areas were located in the Tomé-Açu Mixed Agricultural Cooperative (CAMTA) areas (Table 1) within Tomé-Açu, Pará, Brazil (Figure 2).

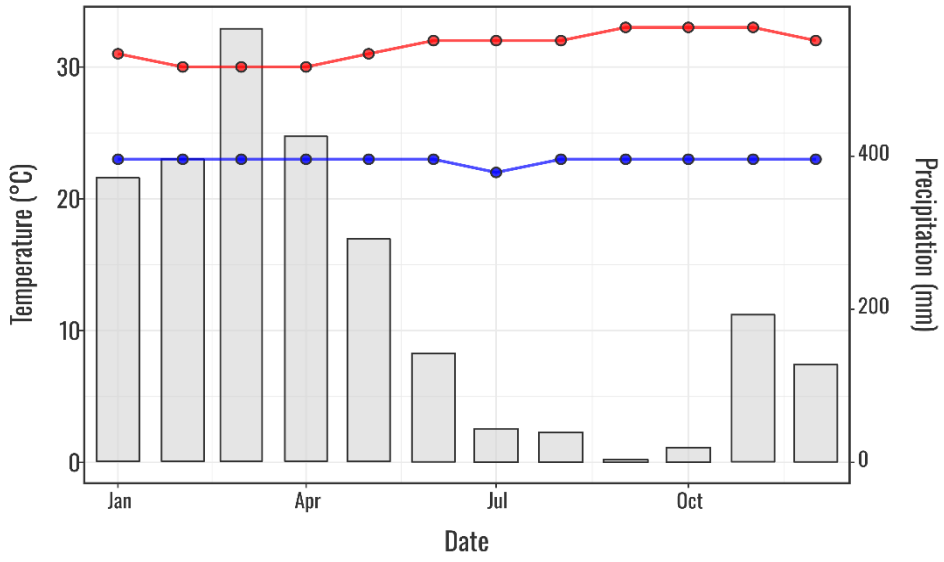

Tomé-Açu 3730881 conventional station data (Tomé-Açu, PA) obtained through the Instituto Nacional de Meteorologia (INMET) and Agência Nacional de Águas e Saneamento Básico (ANA)

Figure 2. Total accumulated precipitation and average monthly temperature in Tomé-Açu during 2023

The region's climate is identified as Af, according to Köppen's climate classification, and characterized as tropical without dry season (Alvares et al., 2013; Pacheco; Bastos, 2001). In 2023, the Tomé-Açu municipality had an average annual of 27.5 ◦C and 2632.8 mm of rainfall (Figure 2). The soils of this region were classified as Oxisol and as "*Latossolo Amarelo Distrófico"* in the Brazilian Soil Classification (Santos et al., 2011). To guarantee a precise comparison between all areas, they all shared a close soil texture and were all once covered by the Amazonia rainforest until forest-to-agriculture conversion and then to either agroforestry or pasture (Figure 4). The details of the land use are presented in Supplementary Table 1.

We also analyzed satellite imagery of the sampling areas to further assess the vegetation cover through the normalized difference vegetation index (NDVI). Like other similar indices, NDVI has been proven to be an efficient tool in assessing chlorophyll content and as a good proxy for vegetation density (Berni et al., 2009; Haboudane et al., 2008, 2004; Le Maire et al., 2008; Myneni et al., 1995). However, in order to compensate for NDVI limitations, we employed the kernel normalized NDVI (Camps-Valls et al., 2021; Zeng et al., 2022) over the 2021-2023 period using the Google Earth Engine platform and Landsat Image Collection.

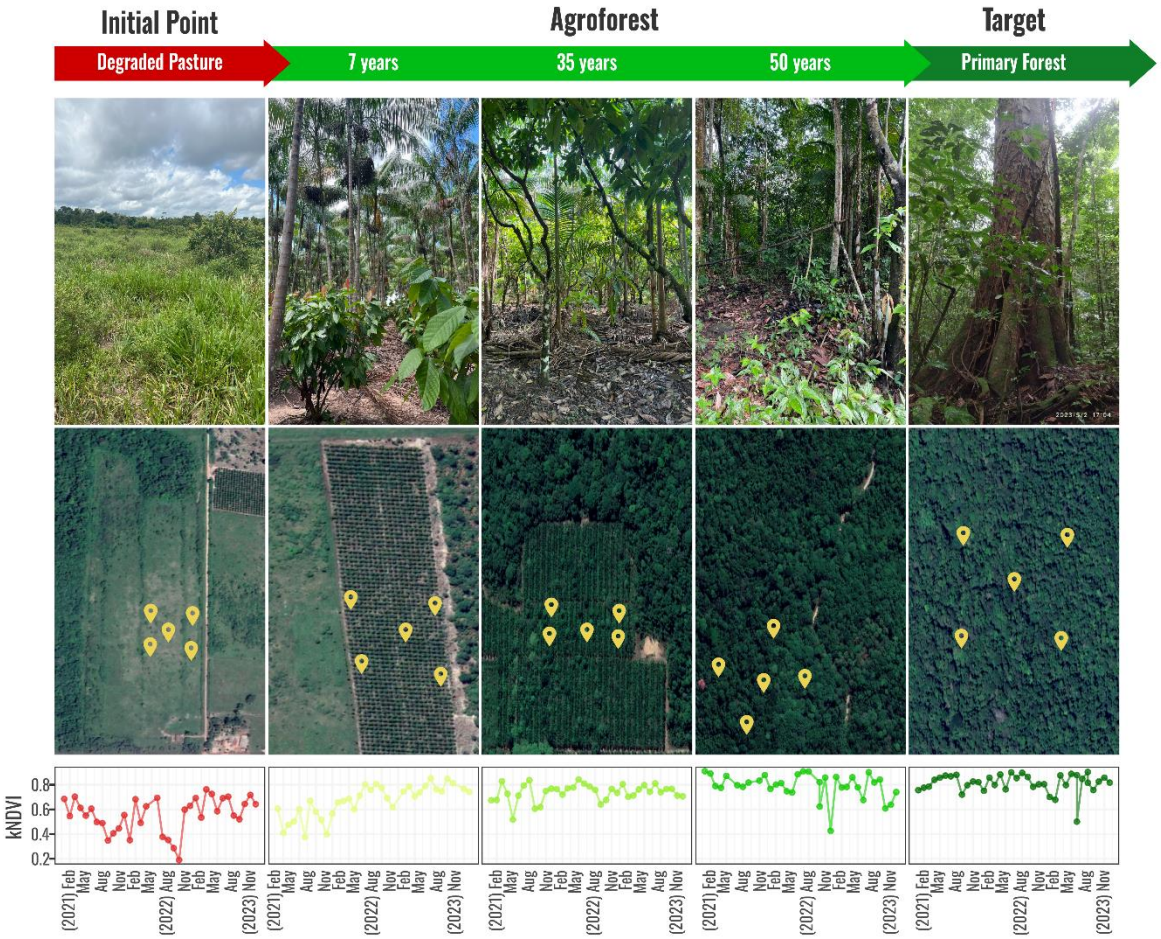

Figure 3. Location of the study sites of long-term agroforest production with 7 (AF-7), 35 (AF-35), and 50 (AR-50) years post agriculture-to-agroforest conversion, primary forest (FOR) and pasture (PAS) within the Amazon biome in the Pará State. Each area is accompanied by their respective temporal series of the normalized difference vegetation index (kNDVI) between 2021 and 2023.

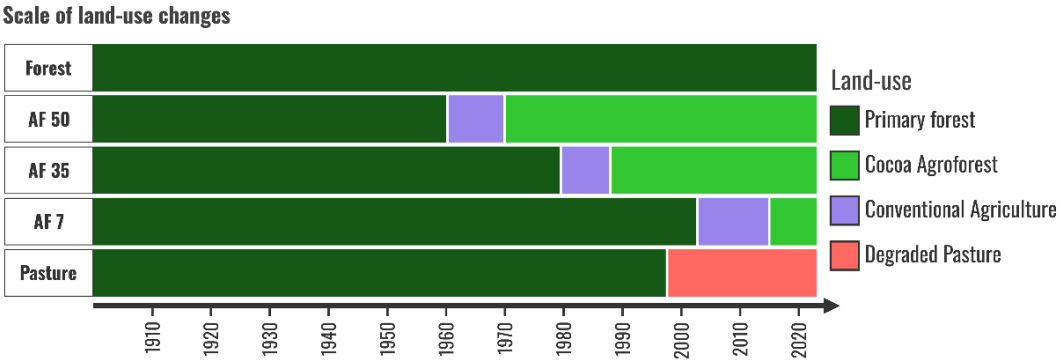

Figure 4. Land use history of the evaluated study areas.

2.2. Litter and soil sampling

Litter and soil sampling was conducted in May 2023, at the end of the wet season, to better represent the highest biological activity in the ecosystem (Venturini et al., 2022). The sampling points were located at least 50 m apart and at a minimum of 30 m from the agroforest borders (Figure 3), while in the pasture and forest sites, the border limit was increased to 100 m. The sampling points were strategically distributed in a square to better represent the entirety of each evaluated area based on its size (Figure 5).

For the litter dry biomass weight and chemical analysis, 25 × 25 cm square plastic frames were used to collect leaf litter material (five points per plot and three replicates per point). All collected material was carefully taken to exclude soil, branches, and wood pieces. The litter was stored in paper bags and dried at 50ºC for 48 hours or until constant weight was achieved. Decaying leaf litter was collected from the forest floor for DNA extraction, carefully avoiding soil and large wood pieces. Leaf litter from different tree species was not distinguished during sampling. Five samples were collected from each point, one from each corner and one from the center (Figure 5), using 50 mL sterile plastic tubes. Samples were then stored and transported in iceboxes to the laboratory for storage in a freezer at -20°C.

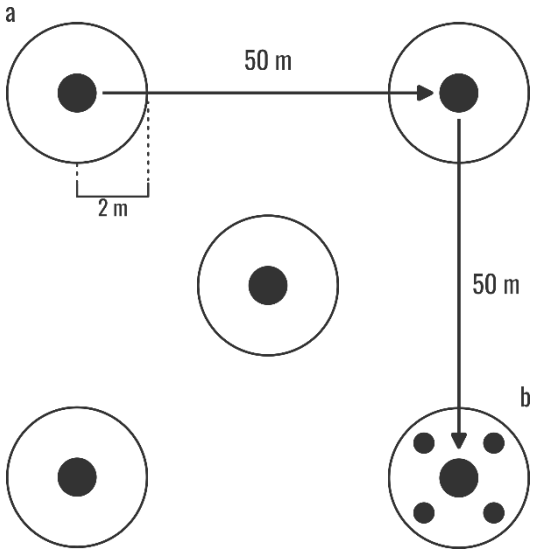

Figure 5. Litter and soil sampling scheme across studied sites. (a) Primary point, (b) Subpoints

Five small trenches (30 × 30 × 30 cm) were excavated at each site to collect undisturbed soil samples. From each trench, undisturbed soil cores were collected in volumetric rings (5 × 5 cm) using a Uhland-type auger for soil physical characterization. Disturbed soil samples from the layers of 0-10, 10-20, and 20-30 cm of the soil were collected directly below the litter sampling points using a Dutch auger. Five soil subsamples were collected at each point from subpoints (Figure 5) and pooled together in order to create a representative sample for chemical, textural, and molecular analysis. The soil-filled volumetric rings were wrapped in plastic film and covered in bubble wrap for transport in order to preserve soil structure. Additionally, 5g of the disturbed soil samples were portioned in cryotubes, immediately frozen in liquid nitrogen, and later stored at -80ºC for subsequent molecular analysis.

2.3. Litter chemical analysis

Leaf litter samples were ground using a knife mill to achieve a particle size lower than 0.25 mm, ensuring sample homogeneity for element content analysis. Five samples were analyzed per plot. The ground litter was analyzed for total macro (P, K, Ca, Mg, and S) and micronutrient (Fe, Cu, Zn, and Mn) content, according to Malavolta et al. (1989). Briefly, the element concentrations were determined from the extract obtained by digesting the litter material in a mixture of HNO_3 and $HClO_4$. P and S were quantified by colorimetry, while other elements were quantified by atomic absorption spectroscopy (PerkinElmer 3100, USA).

2.4. Soil physical and chemical properties

Air-dried soil samples for chemical and texture characterization were grounded and passed through a 2 mm mesh-size sieve. Soil chemical properties (*i.e.*, the soil pH in $CaCl_2$ [pH_{CaCl2}], potential acidity [H + Al], mobile aluminum [Al], available phosphorus [P] and sulfur [S], exchangeable calcium [Ca], magnesium [Mg], and potassium [K], and the concentrations of boron [B], copper [Cu], iron [Fe], manganese [Mn] and zinc [Zn]) were determined following the analytical methods described by van Raij et al. (2001). Soil texture (i.e., clay, silt, and sand contents) was determined according to Teixeira et al. (2017). The texture of all areas was classified according to the USDA Soil Texture Triangle (Supplementary Figure 1).

The undisturbed soil volumetric rings were saturated, placed on a tension table for 24 h under a suction of roughly 5.9 kPa, and weighed to quantify the macroporosity (MaP). Then, soil volumetric rings were dried in an oven at 105 °C for 48 h and weighed again to obtain the microporosity (MiP) and soil bulk density (Bd) according to the methods of Teixeira et al. (2017).

2.5. Litter and soil C and N concentrations and isotopic composition

2.5.1. Litter and bulk soil

Dried and ground litter and soil samples were powdered and sieved for the carbon (C) and nitrogen (N) analysis coupled to their stable isotope ratio ($\delta^{13}C$ and $\delta^{15}N$) determination. Samples were weighed into tin capsules (6 × 8 mm, PN 24,006,400, Thermo Scientific, Bremen, Germany) using a microscale (XP6, Mettler Toledo, Switzerland). The C and N concentrations in litter and soil samples were determined via an automatic elemental analyzer (EA; Flash 2000, Thermo Scientific, Bremen, Germany) coupled to an isotopic ratio mass spectrometry system (Delta V Advantage, Thermo Scientific, Bremen, Germany) through a gas interface (ConFlo IV, Thermo Scientific, Bremen, Germany). The stable isotopes results were expressed as $\delta^{13}C$ and $\delta^{15}N$ (‰) using international standards (Vienna PeeDee Belemnite – V-PDB for C [NBS19 and NBS22] as a reference for ^{13}C values and the composition of atmospheric air for N_2 [IAEA-N1 and IAEA-N2] as a reference for $\delta^{15}N$). The delta values were based on standards (Farquhar et al., 1982) and calculated using the following equation: $\delta X = [(R_{sample} / R_{standard}) - 1]$ multiplied by 1000, where X refers to ^{13}C or ^{15}N, and R_{sample} and $R_{standard}$ are the $^{13}C/^{12}C$ or $^{15}N/^{14}N$ ratios of sample and standard, respectively.

2.5.2. Soil organic matter fractions

The size fractionation method employed in this study is similar to the methodology described in Leuthold et al. (2023), adapted from Cotrufo et al. (2019). Air-dried soils were passed through a 2 mm mesh-size sieve. A 10 g subsample was oven-dried at 60 ºC for 12 h to eliminate residual ambient soil water. Forty milliliters of dilute (0.5 %) sodium hexametaphosphate (SHMP) and two ~ 3 cm glass beads were added to the subsample. The samples were shaken at 250 rpm on a reciprocal shaker for 18 h. The dispersed soil was then rinsed onto a 53 µm sieve, with all material that passed through the sieve considered MAOM (<53 µm) and all material that remained on top of the sieve considered POM (>53 µm). After fractions were dried to a constant weight, the samples were weighed, and their mass recovery was annotated. Mass recoveries varied between 95-105%, which was deemed acceptable. The bulk soil and its respective dried fractions were then powdered using a mortar and pestle (< 100 µm). The C and N concentrations and their stable isotope ratio ($\delta^{13}C$ and $\delta^{15}N$) were then determined through the same methodology mentioned in the 2.5.1 topic above with adaptation to the calibration curves.

2.6. Soil and litter dissolved organic matter

Litter water-extractable organic matter was extracted according to Soong et al. (2014) with modifications. Four grams of litter was extracted with 40 mL of ultrapure water in an orbital shaker at 200 RPM for one hour at 20°C. The resulting mixture was centrifuged at 8000 x g for 10 min, and the supernatant was collected and then filtered through a sterile 0.45 µm syringe filter (Whatman, Maidstone, UK) to obtain the dissolved organic matter.

For the soil water-extractable organic matter, we followed the recommendations of (Jones; Willett, 2005). Briefly, 4 g of unsieved field-moist soil was extracted with 20 mL of ultrapure water in an orbital shaker at 200 RPM for one hour at 20°C. The resulting mixture was centrifuged at 8000 x g for 10 min, and the resulting supernatant was collected and filtered through a sterile 0.22 µm syringe filter (Whatman, Maidstone, UK) to obtain the dissolved organic matter not only from the macropores but from the mesopores and micropores (Chantigny, 2003). The dissolved organic carbon concentrations from litter and soil were assessed by analyzing the total organic carbon concentration with a total organic carbon elemental analyzer (TOC-VCPN, Shimadzu, Japan).

2.7. Laser-induced fluorescence spectroscopy (LIFS) of the soil organic matter and its fractions

Part of the powdered (< 100µm) bulk soil and their respective fractions samples were pelletized (1 cm × 2 mm pellets of approximately 0.5 g) in a hydraulic press in order to reduce matrix effects in the laser-induced fluorescence spectroscopy (LIFS) analysis (Tadini et al., 2021). The LIFS spectra were obtained by a continuous wave laser (20 mJ) with excitation at 405 nm via a mobile prototype system (Santos et al., 2015). The wavelength ranged from 195 to 850 nm, and the maximum emission intensity was 4096 counts. The integration time, mean, and selected boxcar was 500 ms, 3, and 8, respectively (Tadini et al., 2018). We confectioned two pellets for each sample (totaling 500 samples), and the final spectrum was calculated as the average among all the spectrums collected for the same samples. The humification index (H_{LIFS}) was determined as described in Milori et al. (2006) and calculated using the following equation: H_{LIFS} = ESA/C, where ESA refers to emission spectrum area (arbitrary units or a. u.) at 405 nm with 450–800 nm excitation, and C to the total amount of carbon (C%) in the soil sample.

2.8. Litter and soil DNA extraction and purification

The genomic DNA from each soil sample was extracted in triplicate for each point using the DNeasy PowerSoil Pro Kit (Qiagen, Hilden, Germany), following the manufacturer's protocol with necessary alterations to obtain DNA of higher concentration and quality (Venturini et al., 2020). 50 µL from each triplicate was used to generate a pool of 150 µL of DNA, which was then purified using the DNeasy PowerClean Pro Cleanup Kit (Qiagen, Hilden, Germany). The quality of the DNA samples was initially checked on a 1% agarose gel, stained with GelRed™ (Biotium, Fremont, CA, USA) (Brody; Kern, 2004). The extracted DNA quality was determined by the sample absorbance at 230, 260, and 280 nm on a Nanodrop One spectrophotometer (Thermo Fisher Scientific, Middletown, VA, USA). The total DNA was then quantified using a Qubit 4.0 fluorometer (Invitrogen, Carlsbad, USA). The extracted genomic DNA was stored at -20 °C.

The genomic DNA from the litter was extracted using a methodology adapted from that described by (England et al., 2004). Briefly, 5 g of litter was added to sterile tubes with 40 mL of phosphate-buffered saline (PBS). The tubes were shaken at 300 rpm at 4 ºC for 12 hours. Then, the extracts were filtered into a new sterile tube and centrifuged at 10,000 g for 15 minutes. The resulting pellet was used for DNA extraction with the DNeasy PowerSoil Pro

Kit (Qiagen, Hilden, Germany), identical to the previously described method for extracting genomic DNA from soil.

2.9. Quantitative polymerase chain reaction and amplicon sequencing

The total abundance of the selected soil microorganisms (Supplementary Table 2) was measured using Real-Time PCR (qPCR) on a StepOnePlus™ System (Applied Biosystems, Foster City, CA, USA). The qPCR primers are described in Supplementary Table 2. Samples were analyzed in triplicate, with a final volume of 10 µL (5 µL SYBR Green ROX qPCR [Thermo Fisher Scientific], 1 µL of each primer [5 pmol], 1 µL of DNA, and 2 µL of PCR water. All standard curves showed $R^2 > 0.98$. Results were analyzed using StepOnePlus™ Real-Time software version 2.2.2 (Applied Biosystems, Foster City, CA, USA). The results were exported to Excel (Microsoft) and converted to the number of gene copies per gram of soil. The amplicons from the bacterial and fungal communities were amplified from the genomic DNA samples extracted from litter. Polymerase chain reaction (PCR) amplifications were conducted using the same primers from the qPCR analysis (Supplementary Table 2). After amplification, the libraries were quantified in a Qubit 3.0 fluorometer (Invitrogen, Carlsbad, USA) and standardized to equimolar amounts of DNA (50 ng). Sequencing was performed by the Functional Genomics Center (ESALQ/USP), located at the Luiz de Queiroz Campus, using the NextSeq Illumina platform (Illumina, San Diego, USA).

2.10. Bioinformatics

Raw 5.2 M bacterial and 3.2 M fungal raw sequences were analyzed through the nf-core/ampliseq version 2.12.0 (doi: 10.5281/zenodo.1493841) (Straub et al., 2020) of the nf-core collection of workflows (Ewels et al., 2020), utilizing reproducible software environments from the Bioconda (Grüning et al., 2018) and Biocontainers (Da Veiga Leprevost et al., 2017) projects. Data quality was evaluated with FastQC and summarized with MultiQC (Ewels et al., 2016). Cutadapt (Martin, 2011) trimmed primers, and all untrimmed sequences were discarded. Sequences that did not contain primer sequences were considered artifacts. On average, 97% of the 16S rRNA and 99% of the ITS sequences passed the filtering. Adapter and primer-free sequences were processed sample-wise (independent) with DADA2 (Callahan et al., 2016) against the SILVA (v.138.1, Quast et al., 2012) and UNITE (v.9.0, Abarenkov et al., 2024) databases. Further downstream analysis and data visualization were thoroughly carried out in R (v.4.4.1, Abarenkov et al., 2024) using the RStudio platform (RStudio Team, 2020). DADA2

outputs for the bacterial and fungal communities were loaded as a *phyloseq* object (McMurdie and Holmes, 2013).

2.11. Soil health index calculation

The calculation of the Soil Health Index (SHI; Supplementary Table 3) was carried out in three sequential steps following established protocols (Bünemann et al., 2018; Cherubin et al., 2021, 2016b; Rinot et al., 2019; Simon et al., 2022). We first selected indicators (Step I) by identifying a core set of soil properties that are not covariant and collectively reflect the eight fundamental soil functions indicated in Table 3. Upon further soil health assessments, we assembled a minimum dataset of eighteen indicators of chemical (pH, total N, available P, exchangeable K, Ca, and MG, and cation exchange capacity), physical (macroporosity, microporosity, and bulk density), and biological (soil organic C, beta-glucosidase, arylsulfatase, acid phosphatase activities, fungal ITS abundance and diversity, and bacterial 16S rRNA abundance and diversity) soil properties to determine each site performance and if agroforests could restore these indicators to levels observed in primary forests.

Each indicator was selected based on its documented relevance to one or more of the eight functions (Bieluczyk et al., 2025b, 2023; Cherubin et al., 2021, 2016b). Specifically, soil pH dictates nutrient availability, toxic elements solubility, and microbial viability; N, P, and K, Ca, and Mg concentrations reflect immediate nutrient supply; CEC measures soil nutrient retention capacity; bulk density influences root penetration; pore size distribution controls gas exchange and water flow; and organic carbon serves as the primary energy source for soil biota, affecting biological activity and diversity. To incorporate new insights into biological indicators that are essential for tropical ecosystems, we also included the soil enzymatic activity as a proxy of nutrient cycling and molecular measures of fungal and bacterial abundance and diversity, as recommended by Lehmann et al. (2020) and Bieluczyk et al. (2023).

2.12. Data analysis

All statistical analyses and figures were conducted using R (v.4.4.1). The soil and litter physicochemical and biological attributes and SHI indexes were tested for data normality and homogeneity through the Shapiro-Wilk and Bartlett tests. Data was then subject to variance analysis through the Kruskal–Wallis test, followed by Dunn's post hoc ($p \leq 0.05$). Litter and soil chemical dissimilarity were also assessed and visualized through Non-metric Multidimensional Scaling (NMDS) using the Gower distance matrix through the *vegan* and

ggplot2 packages (Oksanen et al., 2020; Wickham; Chang, 2016). Environmental vectors were also fitted into the NMDS plot using the envfit analysis implemented in the *vegan* package.

The ASV tables generated in section 2.10 were loaded as *phyloseq* objects separately for Bacteria and Fungi. Bacterial and fungal relative abundance were calculated and plotted using the *microbiome* package (Lahti et al., 2017). Alpha (Shannon's H') and beta (Bray-Curtis distance) diversity were calculated using the *vegan* package (Oksanen et al., 2020) and visualized through *ggplot2*. The bacterial and fungal dissimilarity matrix was also used for NMDS analysis, with environmental variables fitted into the ordination via envfit and implemented through the *vegan* package. The Linear discriminant analysis Effect Size (LEfSe) was used to indicate microbial biomarkers of land-use changes at the genus taxonomic level (Segata et al., 2011).

3. RESULTS

3.1. Litter and soil chemical composition

Non-metric multidimensional scaling (NMDS) analysis of the litter nutrient profile successfully clustered according to their land uses (Figure 6). NMDS indicated that pasture (PAS) litter was highly dissimilar to other land uses. In contrast, early-stage (AF-7) and mid-stage (AF-35) agroforest were significantly enriched in macronutrients (P, K, Ca, Mg, S) and micronutrients (Fe, B, Zn, Cu) (Table 1), distancing its clusters from other sites. The oldest AFS (AF-50) and FOR sites also formed separate clusters from other land uses, a separation driven mainly by their higher S and dissolved organic carbon concentrations. Finally, the influence land uses types was also confirmed by permutational multivariate analysis of variance (PERMANOVA) of the dissimilarity matrix of chemical data, showing that land uses were responsible for 79% of the variation in the litter layer (Table 2).

The NMDS analysis of the soil profile of the different soil layers (0–10, 10–20, and 20–30 cm) successfully clustered the distinct sites (Figure 6), while the PERMANOVA analysis revealed that the land uses were significantly responsible for 80.3%, 76.6% and 72.9% of the variation found within the 0-10, 10-20, 20-30 cm layers, respectively (Table 2). Across the soil profile, the AF-7 and AF-35 consistently separated from other land uses due to high concentrations of Ca and Mg and elevated pH levels compared to PAS and FOR sites, especially at the soil surface (0-10 cm) layer. PAS sites mimicked the trends observed in their correspondent litter layer and were highly depleted in most analyzed elements. In contrast, while not as heavily enriched as AF-7 and AF-35 sites, AF-50 maintained a moderate concentration of most nutrients. FOR soils were also heavily depleted in base cations and presented the lowest pH of all sites (Table 3), with their high exchangeable Al and Fe concentrations being the major components of the dissimilarity of this site to other land uses (Figure 6). Curiously, the dissimilarity between the chemical profiles of all sites diminished with increasing soil depth. AFS age has shifted from high pH and base-cation saturation in AF-7 toward macro and micronutrient concentration peaks in AF-35. Contrastingly, the older AF-50 slowly presented more acidic, lower-cation soils but with higher sulfur and iron cycling at depth, similar to FOR.

Table 1. Litter chemical characterization parameters

Chemical Properties	PAS	AF-7	AF-35	AF-50	FOR
DOC (mg L^{-1})	70.50 ± 58.40 b	49.39 ± 16.20 b	76.65 ± 23.30 b	262.5 ± 40.90 a	190.4 ± 116.30 a
N (g kg^{-1})	73.4 ± 3.7 d	134.8 ± 6.1 c	171.6 ± 2.4 c	171.0 ± 4.5 b	188.4 ± 3.2 a
P (g kg^{-1})	0.35 ± 0.13 b	0.74 ± 0.10 a	0.70 ± 0.06 a	0.75 ± 0.11 a	0.28 ± 0.15 b
K (g kg^{-1})	0.65 ± 0.17 ab	1.78 ± 0.21 a	0.88 ± 1.63 ab	0.91 ± 0.31 a	0.41 ± 0.21 b
Ca (g kg^{-1})	2.91 ± 4.67 c	22.65 ± 1.25 a	19.55 ± 4.05 a	15.76 ± 5.22 ab	10.69 ± 2.97 bc
Mg (g kg^{-1})	1.39 ± 0.42 b	3.99 ± 0.67 a	2.92 ± 1.22 ab	2.70 ± 1.16 ab	1.67 ± 1.21 b
S (g kg^{-1})	0.63 ± 0.41 b	1.36 ± 0.18 a	1.27 ± 0.10 ab	1.34 ± 0.17 a	1.42 ± 0.10 a
Fe (mg kg^{-1})	1802.8 ± 561.0 ab	699.5 ± 889.9 bc	2234.7 ± 384.6 a	663.7 ± 886.6 c	2306.6 ± 359.6 a
B (mg kg^{-1})	8.56 ± 6.64 c	20.75 ± 2.59 b	32.95 ± 2.61 a	16.99 ± 6.45 bc	20.08 ± 2.72 b
Mn (mg kg^{-1})	132.0 ± 118.7 ab	186.3 ± 41.0 ab	130.0 ± 72.9 b	181.9 ± 34.0 ab	266.1 ± 38.9 a
Zn (mg kg^{-1})	65.75 ± 9.2 bc	90.41 ± 14.41 ab	130.9 ± 19.24 a	49.61 ± 12.24 cd	36.8 ± 15.42 d
Cu (mg kg^{-1})	7.00 ± 4.14 c	137.9 ± 2.96 a	96.08 ± 41.77 a	15.72 ± 87.56 b	12.15 ± 2.12 bc

Values are presented as means ± standard deviation. Lower-case letters indicate the comparison between areas. Sites not sharing the same letter are significantly different from each other (Kruskal-Wallis and Dunn Test; $p < 0.05$). PAS: Degraded pasture; AF-7: Agroforest 7-years; AF-35: Agroforest 35 years ; AF-50: Agroforest 55-years Forest.

Table 2. PERMANOVA table for the chemical profile of the litter and soil layers

Data	Land use		
	R^2	F	***p*-value**
Litter Chemical Properties	0.79162	18.995	**< 0.001**
Soil Chemical Properties (0-10 cm)	0.80341	20.433	**< 0.001**
Soil Chemical Properties (10-20 cm)	0.76657	16.42	**< 0.001**
Soil Chemical Properties (20-30 cm)	0.72944	13.48	**< 0.001**

Bold values indicate statistical significance at $p < 0.05$ (p-value). Distance indexes: Gower (chemical properties). R^2: percentage of the variance explained. F: F-values.

Table 3. Chemical properties of soil in commercial agroforest with seven (AF-7), thirty-five (AF-35), fifty (AF-50), years old, and across the control pasture (PAS) and primary forest (FOR).

Site	pH	P (mg kg^{-1})	K (mmolc kg^{-1})	Ca (mmolc kg^{-1})	Mg (mmolc kg^{-1})	S (mg kg^{-1})	Al (mmolc kg^{-1})	B (mg kg^{-1})	Cu (mg kg^{-1})	Fe (mg kg^{-1})	Mn (mg kg^{-1})	Zn (mg kg^{-1})
0-10 cm												
PAS	4.24 ± 0.11 c	4.49 ± 0.35 b	0.90 ± 0.21 b	5.52 ± 0.64 c	3.08 ± 0.70 c	2.66 ± 1.72 b	5.12 ± 0.81 a	0.15 ± 0.04 c	0.21 ± 0.05 b	135.30 ± 26.98 b	3.50 ± 2.34 a	2.00 ± 0.63 bc
AF-7	5.41 ± 0.42 a	32.81 ± 26.85 b	1.88 ± 0.36 a	25.79 ± 8.95 b	11.04 ± 4.44 a	4.68 ± 0.78 b	0 ± 0 c	0.34 ± 0.02 b	0.48 ± 0.2 b	60 ± 19.15 c	3.07 ± 0.63 ab	2.2 ± 0.82 b
AF-35	5.2 ± 0.23 a	87.57 ± 31.16 a	1.49 ± 0.39 b	43.9 ± 11.4 a	12.96 ± 1.94 a	11.1 ± 4.51 a	0 ± 0 c	0.57 ± 0.07 a	1.85 ± 0.86 a	199.75 ± 60 ab	2.87 ± 0.84 ab	6.80 ± 3.2 a
AF-50	4.12 ± 0.31 b	10.31 ± 6.89 b	0.92 ± 0.15 b	10.46 ± 5.48 c	5.97 ± 5.19 b	5.02 ± 1.65 b	8.5 ± 3.14 b	0.18 ± 0.05 c	1.77 ± 0.36 a	223.9 ± 41.21 a	1.7 ± 0.84 bc	0.52 ± 0.2 bc
FOR	3.6 ± 0.1 c	5.25 ± 0.36 b	0.89 ± 0.04 b	3.25 ± 1.42 c	1.61 ± 0.36 c	14.56 ± 2.03 a	19.5 ± 3.46 a	0.38 ± 0.12 b	0.17 ± 0.04 b	238.35 ± 57.46 a	0.63 ± 0.07 c	0.38 ± 0.13 c
10-20 cm												
PAS	4.04 ± 0.09 b	2.69 ± 0.48 b	0.7 ± 0.08 b	3.02 ± 1.60 b	1.24 ± 0.63 bc	2.44 ± 1.16 c	6.5 ± 1.14 b	0.15 ± 0.02 b	0.11 ± 0.05 b	70.25 ± 7.98 b	1.83 ± 0.82 a	0.58 ± 0.27 b
AF-7	5.12 ± 0.3 a	5.58 ± 4.22 b	1.6 ± 0.57 a	10.52 ± 4.22 b	4.86 ± 1.36 b	2.95 ± 0.79 c	1.63 ± 1.57 c	0.27 ± 0.01 a	0.16 ± 0.07 b	60.7 ± 18.34 b	1.37 ± 0.59 ab	0.41 ± 0.34 b
AF-35	5.01 ± 0.12 a	65.38 ± 35.81 a	1.06 ± 0.12 b	25.65 ± 12.84 a	9.04 ± 0.82 a	8.66 ± 3.64 ab	1.00 ± 1.37 c	0.36 ± 0.06 a	0.99 ± 0.45 a	161.95 ± 54.25 a	1.43 ± 0.42 ab	2.72 ± 1.22 a
AF-50	4.1 ± 0.26 b	9.95 ± 12.1 b	0.72 ± 0.06 b	5.73 ± 3.39 b	3.9 ± 3.06 bc	5.04 ± 1.39 bc	9.25 ± 3.17 b	0.13 ± 0.04 b	1.40 ± 0.68 a	144.05 ± 28.42 a	0.73 ± 0.38 ab	0.32 ± 0.11 b
FOR	3.69 ± 0.11 c	3.09 ± 0.78 b	0.78 ± 0.12 b	3.08 ± 0.49 b	0.68 ± 0.22 c	11.05 ± 1.43 a	17.88 ± 2.24 a	0.27 ± 0.11 a	0.08 ± 0.03 b	124.8 ± 62.33 ab	0.2 ± 0.07 b	0.14 ± 0.03 b
30-20 cm												
PAS	4.02 ± 0.08 b	1.52 ± 0.46 b	0.64 ± 0.08 b	3.00 ± 1.71 b	0.91 ± 0.46 b	2.34 ± 1.43 c	7.5 ± 1.17 b	0.13 ± 0.02 b	0.09 ± 0.03 b	47.65 ± 12.76 b	1.43 ± 0.53 a	0.47 ± 0.3 a
AF-7	4.65 ± 0.4 a	2.09 ± 0.67 b	1.18 ± 0.41 a	4.78 ± 3.46 b	3.32 ± 0.69 ab	6.73 ± 3.34 abc	3.75 ± 2.34 c	0.3 ± 0.03 a	0.19 ± 0.06 b	44.75 ± 19.75 b	0.73 ± 0.37 a	0.29 ± 0.25 a
AF-35	4.68 ± 0.14 a	52.39 ± 27 a	0.97 ± 0.13 ab	17.39 ± 7.44 a	6.51 ± 0.84 a	10.38 ± 7.95 ab	3.75 ± 1.33 c	0.38 ± 0.1 a	0.61 ± 0.15 ab	131.9 ± 26.28 a	0.9 ± 0.38 a	1.29 ± 0.35 a
AF-50	4.03 ± 0.24 b	7.58 ± 9.27 b	0.64 ± 0.03 b	6.21 ± 3.12 b	2.75 ± 1.93 ab	5.38 ± 1.24 bc	10.00 ± 3.28 b	0.12 ± 0.04 b	0.88 ± 0.58 a	103.4 ± 24.73 ab	0.3 ± 0.14 a	0.39 ± 0.5 a
FOR	3.8 ± 0.07 c	2.29 ± 0.52 b	0.68 ± 0.09 b	3.12 ± 1.18 b	0.64 ± 0.28 b	11.77 ± 1.19 a	16.75 ± 0.81 a	0.19 ± 0.05 b	0.09 ± 0.03 b	86.45 ± 36.83 ab	0.17 ± 0.00 a	0.18 ± 0.07 a

Values are presented as means ± standard deviation. Lower-case letters indicate the comparison between areas. Sites not sharing the same letter are significantly different from each other (Kruskal-Wallis and Dunn Test; $p < 0.05$). PAS: Degraded pasture; AF-7: Agroforest 7-years; AF-35: Agroforest 35 years ; AF-50: Agroforest 55-years Forest.

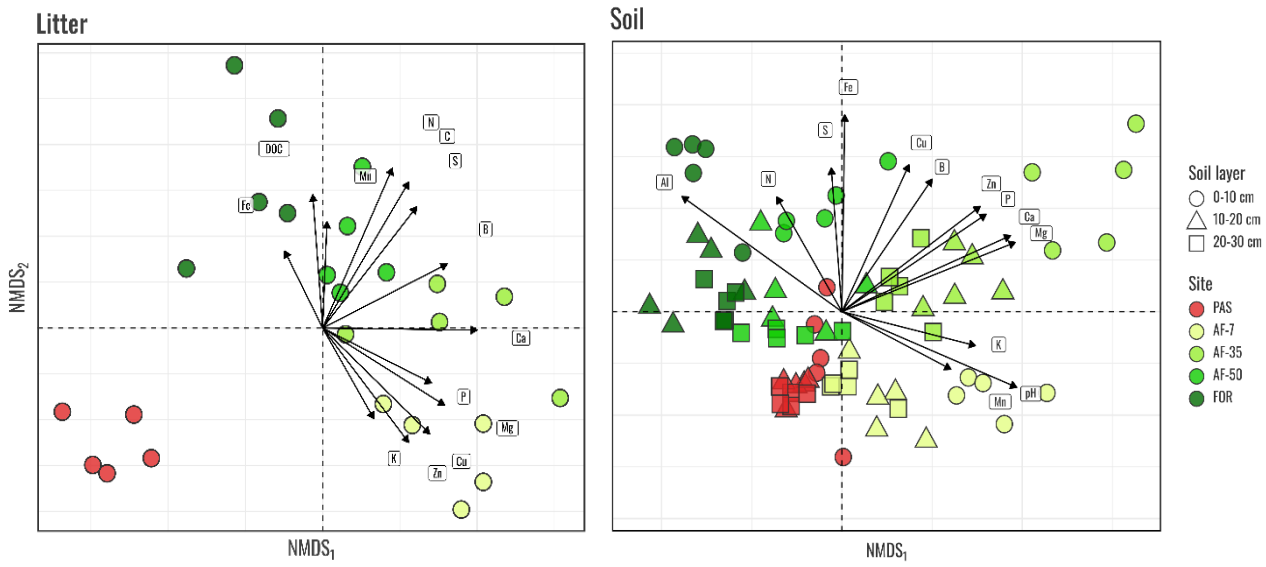

Figure 6. Non-metric multidimensional scaling (NMDS) based on the Gower distance matrix of the litter and soil chemical profile and from five land use systems: pasture (PAS), 7 years old AFS (AF-7), 35 years old AFS (AF-35), 50 years old AFS (AF-50) and native forest (FOR).

3.2. C and N stocks and their isotopic signature

3.2.1. Litter layer

Litter dry biomass increased across the successional land-use gradient, ranging from 5.4 to 17.9 Mg ha^{-1} (Figure 7; Table 4). PAS and AF-7 accumulated 5.4 and 5.7 M g of litter per hectare, respectively, with no significant differences. Contrastingly, AF-35 and AF-50 had significantly higher litter biomass stocks, averaging 7.5 and 13.6 Mg ha^{-1}, while primary forests boasted the highest stocks of 17.9 Mg ha^{-1}. Both C and N concentrations in the litter increased with AFS age. Litter derived from PAS sites averaged 400 g C kg^{-1} and 7.3 g N kg^{-1}, concentrations consistently lower than those found even in the young AF-7 (Figure 8; Table 4). Litter C and N increased as AFS aged, reaching 454.2 g C kg^{-1} and 18.84 g N kg^{-1} in AF-50 and peaking in FOR sites. Consequently, C/N ratios declined from 54.6 in PAS to 24.1 in AF-50 (55 yr) and 26.9 in FOR. The $\delta^{13}C$ of pasture litter (–15.08 ‰) was enriched relative to all agroforest and forest sites, averaging between –30.9 to –31.0 ‰. Litter $\delta^{15}N$ remained low in PAS, AF-7, and AF-35 sites, ranging from 0.89‰ to 1.27‰, while AF-50 and FOR sites had significantly higher enrichment in its heavier isotope, reaching 3.13 ‰ in AF-50 and 2.60 ‰ in FOR.

Table 4. Carbon (C) and nitrogen (N) contents, C/N ratio, and stable isotopic abundance of carbon ($\delta^{13}C$) and nitrogen ($\delta^{15}N$) in the litter and in the 0–10, 10–20, and 20–30 cm soil layers of Amazon agroforest at seven (AF-7), thirty-five (AF-35), fifty (AF-50) years of age, and in a primary forest (FOR) and degraded pasture (PAS).

Site	C (g kg^{-1})	N (g kg^{-1})	C:N	$\delta^{13}C$ (‰)	$\delta^{15}N$ (‰)
Litter					
PAS	400 ± 3.16 c	7.34 ± 0.36 d	54.61 ± 2.81 a	-15.08 ± 0.64 a	1.27 ± 0.24 b
AF-7	442.8 ± 3.7 b	13.48 ± 0.61 c	32.89 ± 1.24 b	-30.90 ± 0.59 b	1.22 ± 0.17 b
AF-35	452.2 ± 2.86 ab	17.16 ± 0.24 b	26.36 ± 0.5 c	-30.84 ± 0.19 b	0.89 ± 0.47 b
AF-50	454.2 ± 4.66 a	18.84 ± 0.32 a	24.11 ± 0.32 d	-30.45 ± 0.48 b	3.13 ± 0.41 a
FOR	460.6 ± 3.05 a	17.1 ± 0.45 b	26.95 ± 0.72 c	-31.03 ± 0.12 b	2.60 ± 0.58 a
0-10 cm					
PAS	16.59 ± 11.5 c	1.47 ± 0.98 c	11.13 ± 0.38 b	-18.4 ± 1.34 a	6.71 ± 0.36 b
AF-7	19.28 ± 11.29 c	1.38 ± 0.74 c	13.77 ± 0.83 a	-24.1 ± 0.95 b	6.90 ± 0.51 b
AF-35	22.11 ± 5.03 bc	1.77 ± 0.4 bc	12.48 ± 0.15 ab	-28.57 ± 0.41 c	6.65 ± 0.55 b
AF-50	31.47 ± 4.94 b	2.31 ± 0.4 b	13.63 ± 0.28 a	-28.47 ± 0.23 c	8.12 ± 0.48 a
FOR	45.55 ± 14.64 a	3.21 ± 0.83 a	14.00 ± 0.88 a	-28.56 ± 0.18 c	7.93 ± 0.64 a
10-20 cm					
PAS	9.44 ± 6.48 b	0.81 ± 0.57 b	11.73 ± 0.49 a	-19.34 ± 1.22 a	7.84 ± 0.44 cd
AF-7	12.7 ± 1.58 b	0.99 ± 0.17 b	12.93 ± 0.71 a	-24.45 ± 1.60 b	8.55 ± 0.42 d
AF-35	14.11 ± 2.04 b	1.13 ± 0.15 b	12.52 ± 1.01 a	-26.63 ± 0.52 c	9.72 ± 0.75 a
AF-50	14.99 ± 2.94 ab	1.16 ± 0.22 ab	12.89 ± 0.61 a	-28.02 ± 0.34 cd	7.42 ± 0.45 bc
FOR	25.17 ± 2.78 a	1.95 ± 0.13 a	12.92 ± 0.68 a	-27.95 ± 0.18 d	9.25 ± 0.59 ab
20-30 cm					
PAS	8.79 ± 6.05 b	0.72 ± 0.37 b	11.66 ± 1.59 a	-22.54 ± 0.66 a	9.51 ± 0.71 bc
AF-7	6.59 ± 2.12 b	0.56 ± 0.17 b	11.72 ± 0.72 a	-25.22 ± 1.67 b	10.02 ± 0.79 b
AF-35	7.99 ± 2.22 b	0.65 ± 0.13 b	12.22 ± 1.25 a	-26.33 ± 0.36 bc	11.26 ± 0.6 a
AF-50	8.07 ± 1.7 b	0.62 ± 0.07 b	12.94 ± 1.19 a	-27.08 ± 0.41 cd	8.95 ± 0.55 c
FOR	22.07 ± 6.22 a	1.74 ± 0.35 a	12.56 ± 0.97 a	-27.8 ± 0.43 d	9.72 ± 0.83 bc

Mean values followed by the same lowercase letter do not differ significantly according to Dunn's test ($p \leq 0.05$).

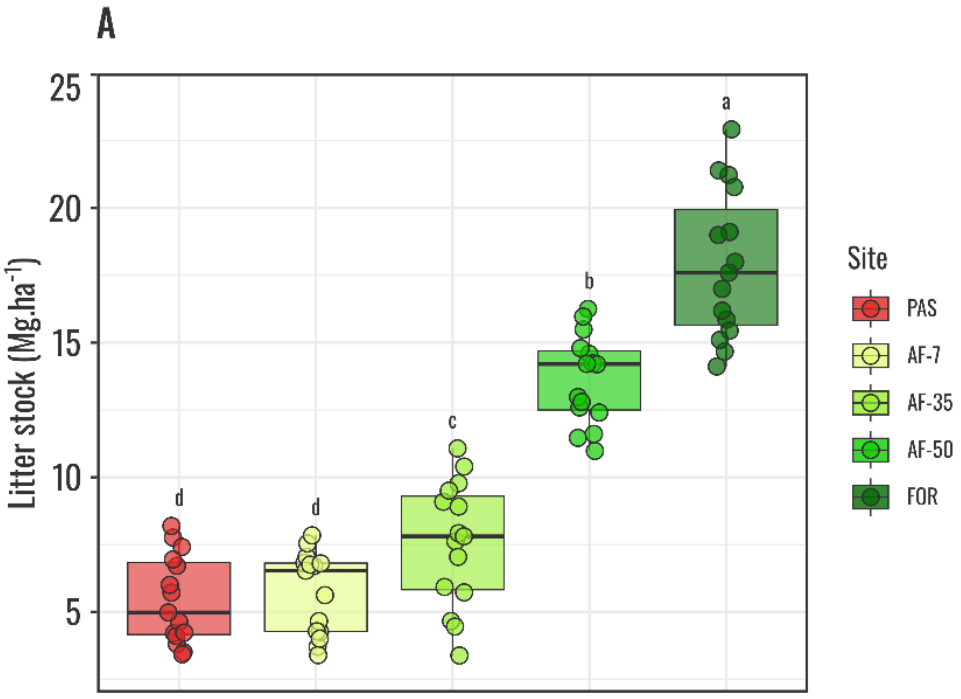

Figure 7. Dry mass of the litter layer from agroforests (AF-7, AF-35, and AF-50), primary forest (FOR), and pasture (PAS). Mean values followed by the same lowercase letter do not differ significantly according to Dunn's test ($p \leq 0.05$).

3.2.2. Soils

In soils, total C and N contents increased with AFS succession, albeit this growth was significantly attenuated with soil depth (Table 4). The topsoil layer (0-10 cm) was the most influenced by the land uses, with PAS and AF-7 averaging 16.6 and 19.3 g C kg-1, respectively, with no significant difference between them. The same pattern was observed for N content, with no significant difference between the two sites. In contrast, at the AF-35 and AF-50, C and N concentrations significantly rose to 22.1 g C kg-1 and 1.8 g N kg-1 at AF-35 and 31.5 g C kg-1 and 2.7 g N kg-1 at the AF-50, reaching levels close to those found in FOR sites (45.5 g C kg-1 and 3.21 g N kg-1). The same progression was observed in the 10-20 and 20-30 cm layers for C and N, albeit with less distinction between land uses (Table 4). At the second soil layer, C concentrations did not differ between the PAS, AF-7, and AF-35 sites, while AF-50 reached intermediate values between FOR and the other land uses. Most sites did not differ at the deepest soil layer, with only the FOR site reaching significantly higher C concentrations (22.0 g C kg-1). Nitrogen (N) concentrations followed the patterns observed for C across all three soil layers.

The $\delta^{13}C$ in all agroforest and forest sites ranged from -24 to -28 ‰, characteristics of soils under long-term C_3 plant cover (Table 4). In contrast, the PAS sites ranged from -18 in the top layer to -22 in the deepest layer. Contrastingly, the $\delta^{15}N$ progressively increased in the three AFS and the FOR sites as they became enriched in the heavier ^{15}N isotope (Table 4). $\delta^{15}N$ also increased with soil depth, reaching values as high as 11.3 ‰ in the AF-35. Primary forests contained by far the highest C stocks from the litter to the 30 cm layer, while both PAS and AF-7 equally had the lowest stocks (Figure 8). Interestingly, the AF-35 boasted higher total C stocks, which by AF-50 were significantly higher in both the 0-10 and 20-30 cm layers. While not close to the total C stock in the FOR litter and soils, AF-35 and AF-50 steadily increased C stocks from the litter to the 10-20 cm layer.

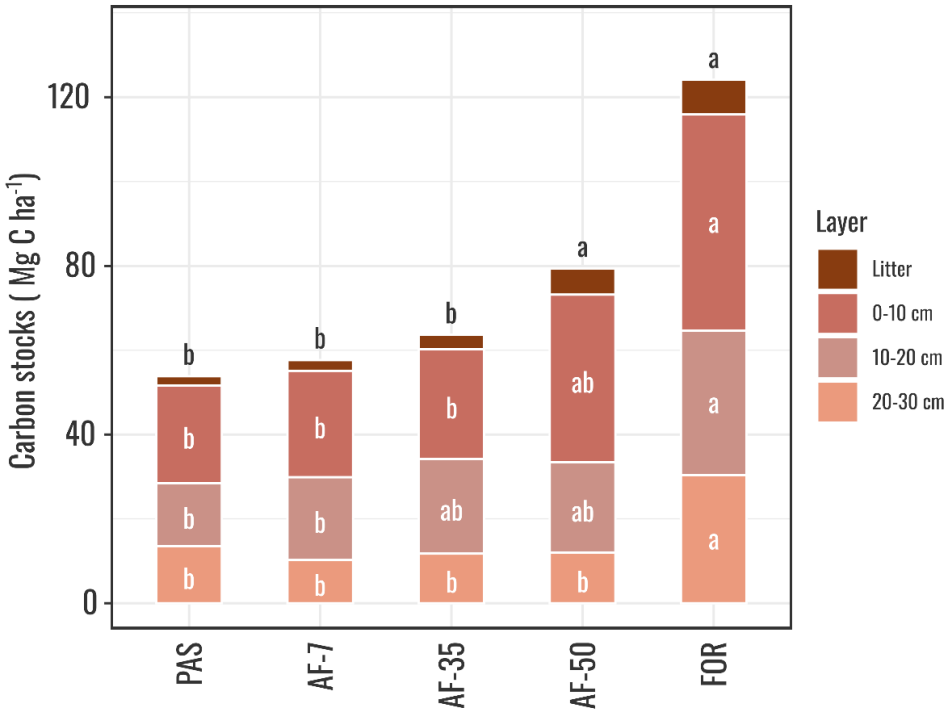

Figure 8. Soil carbon stocks of the litter and the 0–10 cm, 10–20 cm, and 20–30 cm soil layers from agroforests (AF-7, AF-35, and AF-50), primary forest (FOR) and pasture (PAS) in Eastern Amazon. Mean values followed by the same lowercase letter do not differ significantly according to Dunn's test ($p \leq 0.05$).

3.2.3. Particulate and mineral-associated soil organic matter fractions

The land-use succession from PAS to AFS continuously increased C concentration in particulate organic matter (POM) and mineral-associated organic matter (MAOM) across measured samples. The C concentration of the SOM fractions also followed a top-to-bottom pattern of increase, as most of the carbon in both fractions was in the 0-10 cm layer (Figure 9). The conversion of these values in total C stocks showed that in the soil surface (0-10 cm), the AF-35 and AF-50 accumulated 14.7 and 17.0 Mg C ha^{-1} in the MAOM fraction and 2.3 and 3.8 Mg C ha^{-1} in the POM fraction, a 48% and 71% increase in MAOM stocks, and an 81% and 197% increase in POM compared to PAS sites. In the subsoil layers (10-20 and 20-30 cm), the FOR site had substantially higher C stocks in the MAOM fraction, while all other land uses did not significantly differ. The same pattern was observed in the POM fraction, with shifts in land use having almost no effect on C accumulation.

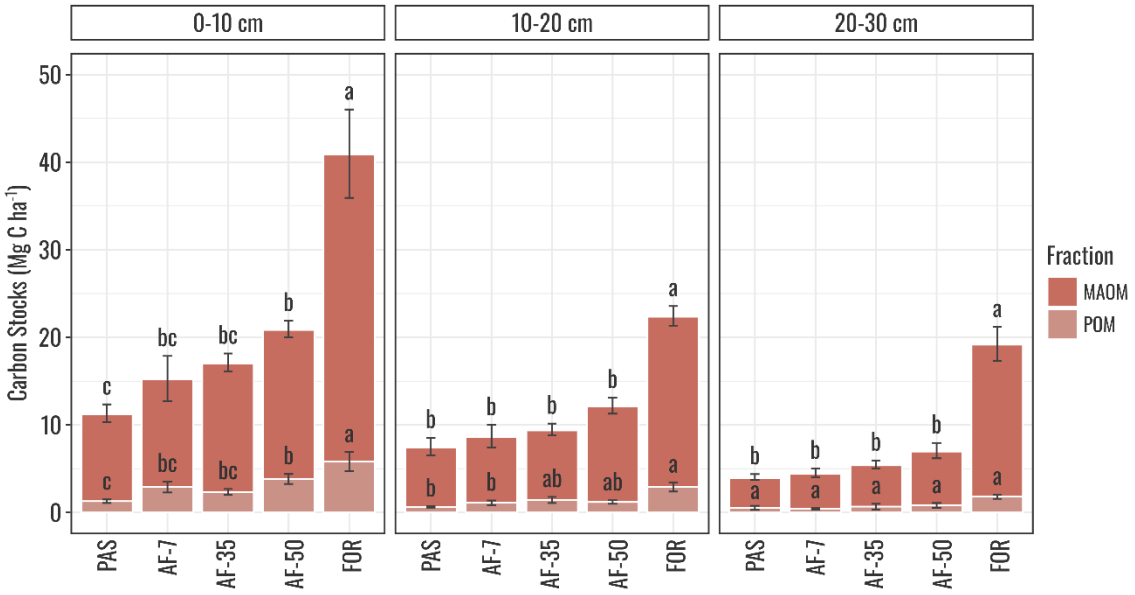

Figure 9. Particle-size fractionation of soil organic matter across the 0–10 cm, 10–20 cm, and 20–30 cm soil layers from agroforests (AF-7, AF-35, and AF-50), primary forest (FOR) and pasture (PAS) in Eastern Amazon. Mean values followed by the same lowercase letter do not differ significantly according to Dunn's test ($p \leq 0.05$).

The C and N concentrations in the POM and MAOM fractions responded differently to land use succession (Table 5, Table 6). In the POM fraction, the C and N concentrations from PAS and AFS sites did not differ in any soil layer, while FOR sites boasted extraordinarily high concentrations. In the MAOM fraction, C concentration only varied in the 0-10 cm soil layer

and responded independently of the land use succession, with AF-7 boasting the highest concentration (54.8 g kg^{-1}) and AF-35 and FOR the lowest. In contrast, N concentrations were only significantly different in FOR sites in the 0-10 cm layer, while all other land uses did not differ.

Table 5. Carbon (C) and nitrogen (N) contents, C/N ratio, and stable isotopic abundance of carbon ($\delta^{13}C$) and nitrogen ($\delta^{15}N$) in particulate organic matter (POM) at 0–10, 10–20, and 20–30 cm soil layers of Amazon agroforest at seven (AF-7), thirty-five (AF-35), fifty (AF-50) years-old, and in a primary forest (FOR) and degraded pasture (PAS).

Site	C (g kg^{-1})	N (g kg^{-1})	C:N	$\delta^{13}C$ (‰)	$\delta^{15}N$ (‰)
0-10 cm					
PAS	1.63 ± 0.53 b	0.08 ± 0.02 b	20.83 ± 2.63 a	-20.64 ± 2.75 a	5.79 ± 0.36 a
AF-7	3.75 ± 1.65 b	0.16 ± 0.07 b	24.27 ± 2.79 a	-26.01 ± 0.92 b	5.18 ± 0.32 a
AF-35	3.54 ± 1.01 b	0.18 ± 0.05 b	20.02 ± 1.12 a	-29.19 ± 0.27 c	5.05 ± 0.67 a
AF-50	5.68 ± 1.74 b	0.23 ± 0.07 b	25.26 ± 3.44 a	-28.89 ± 0.25 c	6.08 ± 0.48 a
FOR	29.3 ± 14.72 a	1.38 ± 0.83 a	22.34 ± 2.55 a	-29.31 ± 0.26 c	5.37 ± 0.46 a
10-20 cm					
PAS	0.81 ± 0.17 b	0.03 ± 0.00 b	25.47 ± 4.72 b	-22.51 ± 1.87 a	6.23 ± 0.69 a
AF-7	1.54 ± 0.82 b	0.04 ± 0.02 b	35.61 ± 12.25 ab	-25.87 ± 0.48 b	6.94 ± 1.03 a
AF-35	1.95 ± 0.62 b	0.06 ± 0.02 b	30.94 ± 5.49 ab	-28.18 ± 0.47 bc	5.15 ± 0.93 a
AF-50	2.17 ± 1.03 b	0.05 ± 0.01 b	44.19 ± 15.97 a	-27.26 ± 0.34 bc	6.07 ± 1.45 a
FOR	12.98 ± 6.64 a	0.53 ± 0.22 a	24.26 ± 1.97 b	-28.83 ± 0.32 c	5.57 ± 1.85 a
20-30 cm					
PAS	0.66 ± 0.64 b	0.02 ± 0.01 a	31.91 ± 15.02 ab	-23.94 ± 0.79 a	4.73 ± 1.17 bc
AF-7	0.55 ± 0.25 b	0.02 ± 0.01 a	25.83 ± 5.19 b	-26.18 ± 0.5 b	6.67 ± 0.41 a
AF-35	1.41 ± 1.03 b	0.03 ± 0.01 a	42.31 ± 11.17 a	-27.86 ± 0.53 b	3.78 ± 1.58 c
AF-50	1.02 ± 1.03 b	0.02 ± 0.01 a	38.34 ± 16.34 ab	-26.77 ± 0.44 b	5.54 ± 1.69 ab
FOR	7.81 ± 1.78 a	0.34 ± 0.1 a	23.23 ± 1.55 b	-28.62 ± 0.22 c	6.18 ± 0.53 ab

Mean values followed by the same lowercase letter do not differ significantly according to Dunn's test ($p \leq 0.05$).

The $\delta^{13}C$ and $\delta^{15}N$ signals provided further insights into the soil organic matter dynamics across land uses and soil layers (Table 5, Table 6). The MAOM was slightly enriched in ^{13}C, with higher $\delta^{13}C$ in all land uses than POM. Across all land uses, $\delta^{13}C$ was also enhanced with soil depth, with consistent enrichment in ^{13}C in deeper layers in POM and MAOM. The $\delta^{13}C$ also constantly decreased from PAS through the AFS succession, reaching its lowest values in FOR sites in both fractions. The $\delta^{15}N$ in the POM fraction did not display high variation between land uses across the soil profile. In contrast, the MAOM was progressively enriched in ^{15}N as land use succession progressed.

Table 6. Carbon (C) and nitrogen (N) contents, C/N ratio, and stable isotopic abundance of carbon ($\delta^{13}C$) and nitrogen ($\delta^{15}N$) in the mineral associated organic matter (MAOM) at 0–10, 10–20, and 20–30 cm soil layers of Amazon agroforest at seven (AF-7), thirty-five (AF-35), fifty (AF-50) years-old, and in a primary forest (FOR) and degraded pasture (PAS).

Site	C (g kg^{-1})	N (g kg^{-1})	C:N	$\delta^{13}C$ (‰)	$\delta^{15}N$ (‰)
0-10 cm					
PAS	46.9 ± 6.01 ab	4.36 ± 0.53 a	10.76 ± 0.34 b	-18.15 ± 1.34 a	7.01 ± 0.19 b
AF-7	54.84 ± 10.00 a	4.27 ± 0.76 a	12.84 ± 0.57 a	-23.4 ± 1.25 b	7.13 ± 0.29 b
AF-35	43.17 ± 5.83 b	3.74 ± 0.45 ab	11.53 ± 0.42 ab	-28.34 ± 0.34 c	6.89 ± 0.72 b
AF-50	51.86 ± 4.26 ab	4.07 ± 0.41 ab	12.77 ± 0.43 a	-28.25 ± 0.18 c	8.71 ± 0.28 a
FOR	43.97 ± 12.99 b	3.36 ± 0.75 b	12.91 ± 0.94 a	-28.43 ± 0.59 c	8.39 ± 0.74 a
10-20 cm					
PAS	30.13 ± 3.14 a	2.67 ± 0.27 a	11.3 ± 0.25 a	-19.18 ± 1.2 a	7.56 ± 0.4 c
AF-7	26.76 ± 7.17 a	2.19 ± 0.53 a	12.15 ± 0.46 a	-23.92 ± 1.6 b	8.71 ± 0.36 b
AF-35	28.17 ± 6.32 a	2.32 ± 0.53 a	12.14 ± 0.35 a	-27.68 ± 0.28 c	7.48 ± 0.62 c
AF-50	22.71 ± 5.12 a	1.92 ± 0.39 a	11.79 ± 0.67 a	-26.34 ± 0.5 c	10.06 ± 0.53 a
FOR	25.36 ± 3.22 a	2.12 ± 0.18 a	11.94 ± 0.52 a	-27.74 ± 0.65 c	9.6 ± 0.42 ab
20-30 cm					
PAS	16.58 ± 5.44 a	1.43 ± 0.29 ab	11.42 ± 1.40 a	-22.41 ± 0.72 a	9.11 ± 0.44 bc
AF-7	14.67 ± 2.78 a	1.31 ± 0.22 ab	11.17 ± 0.56 a	-24.75 ± 1.63 b	10.07 ± 0.58 b
AF-35	14.42 ± 3.18 a	1.16 ± 0.18 ab	12.33 ± 0.88 a	-26.58 ± 0.14 cd	8.77 ± 0.61 c
AF-50	13.18 ± 3.18 a	1.06 ± 0.07 b	12.36 ± 2.30 a	-26.1 ± 0.32 bc	11.13 ± 0.36 a
FOR	22.60 ± 6.12 a	1.89 ± 0.35 a	11.80 ± 0.99 a	-27.8 ± 0.48 d	10.05 ± 1.01 b

Mean values followed by the same lowercase letter do not differ significantly according to Dunn's test ($p \leq 0.05$).

3.3. Dissolved organic carbon

The litter dissolved organic carbon (DOC) showed a clear, non-linear pattern across the successional gradient from the PAS site through successive AFS stages to FOR (Figure 10). PAS sites displayed 70.5 mg L^{-1} of DOC, which decreased (-29.9%) in early AFS (AF-7) to 49.3 mg L^{-1}. Through AFS succession, litter DOC increased by roughly 55.2% from AF-7 to AF-35 (76.6 mg L^{-1}), then increased by 242.4% and plateaued in AF-50 with 185.8 mg L^{-1}.

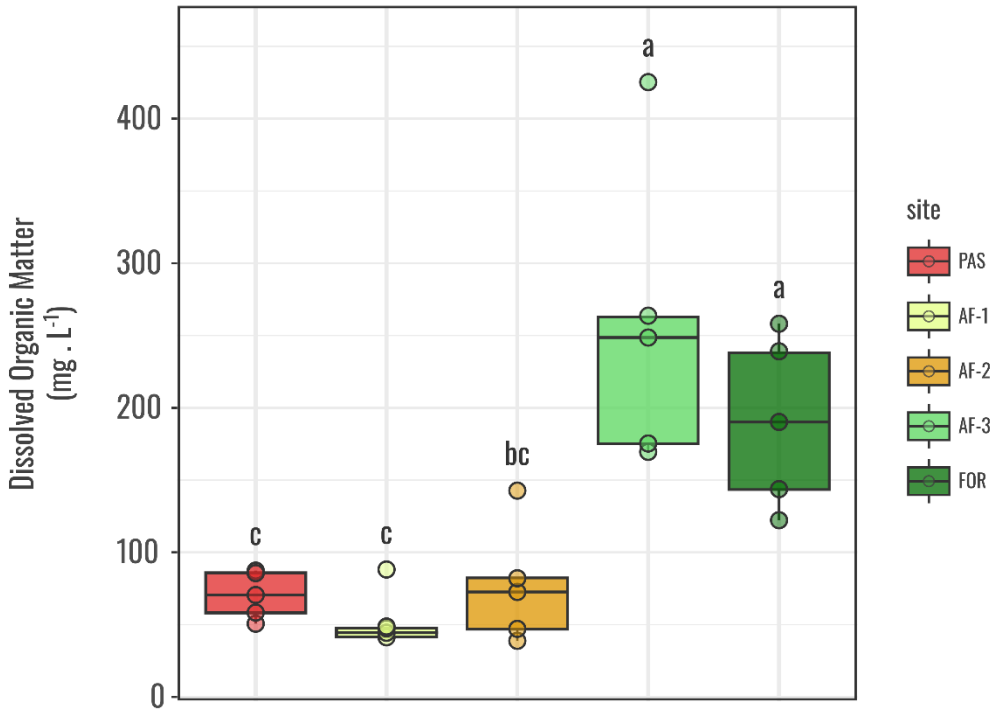

Figure 10. Dissolved organic carbon (DOC) in the litter layer from agroforests (AF-7, AF-35, and AF-50), primary forest (FOR) and pasture (PAS) in Eastern Amazon.

The soil-dissolved organic matter, especially in the surface layer (0-10 cm), displayed a similar pattern to the litter layer (Figure 11). Soil DOC decreased from 36.1 mg L^{-1} in the PAS site to 25.8 mg L^{-1} in AF-7 (-28.5%), then progressively increased to 39.3 mg L^{-1} in AF-35 (52.2%) and 54.4 mg L^{-1} in AF-50 (38.2%). FOR soil DOC (62.7 mg L^{-1}) was also not statistically different from AF-50. In the subsurface layers, soils maintained similar concentrations of DOC as in the soil surface across all land uses, except AF-7, which increased DOC in the 10-20 and 20-30cm layers.

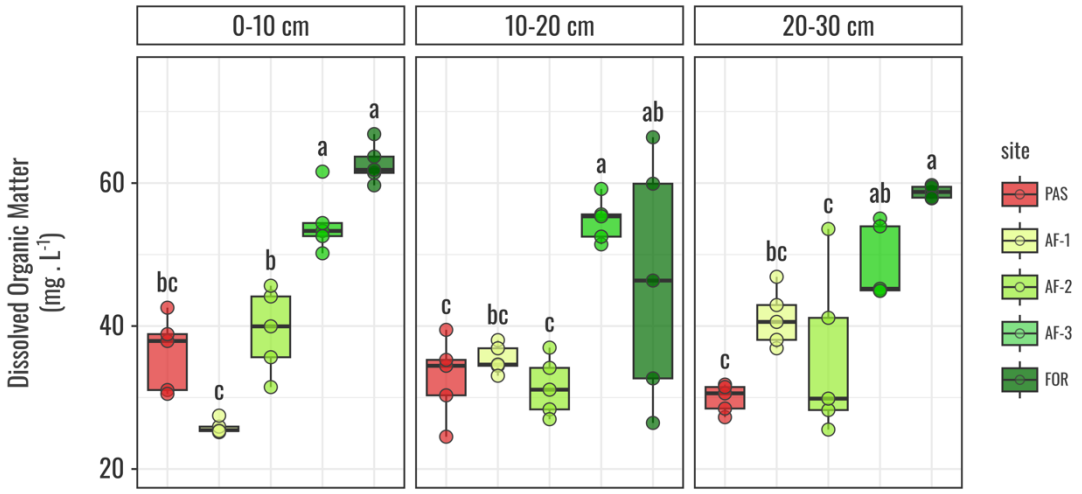

Figure 11. Soil dissolved organic carbon (DOC) in the 0-10, 10-20, and 20-30 cm layers from agroforests (AF-7, AF-35, and AF-50), primary forest (FOR) and pasture (PAS) in Eastern Amazon.

3.4. Laser-induced fluorescence of SOM, POM, and MAOM

The humification index (H_{lifs}) was examined in the bulk soil organic matter (SOM), particulate organic matter (POM), and mineral-associated organic matter (MAOM) across the four successive land-use stage (AF-7, AF-35, AF-50, and FOR) relative to PAS sites (Figure 12). In the surface horizon, bulk SOM H_{lifs} did not differ between PAS and AF-7, declining from AF-7 to AF-35 (-34.6%) and then to AF-50 and FOR (-64.2, -59.1%, respectively). In contrast, at the 10-20 and 20-30 cm layers, bulk SOM H_{lifs} did not differ between PAS, AF-7, and AF-35 but followed the same decrease pattern in the older AFS-50 and FOR sites. The POM and MAOM fractions followed the same pattern observed in bulk SOM at distinct scales, as POM was highly humified and exhibited H_{lifs} values more than ten times higher than bulk SOM and MAOM fractions.

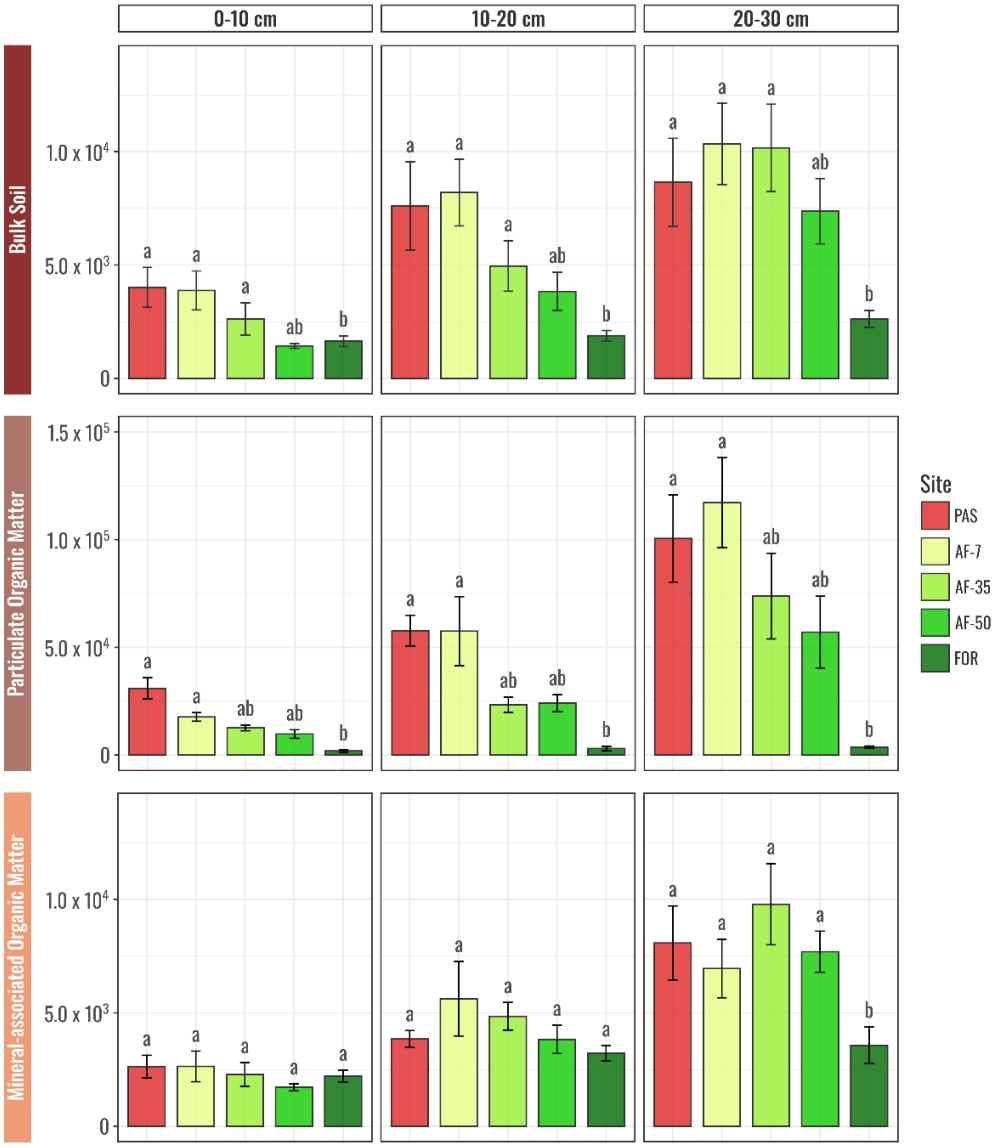

Figure 12. Soil organic matter humification index (H_{LIFS}) from bulk soil organic matter, particulate and mineral-associated organic matter pools for all soil layers and across agroforests (AF-7, AF-35, and AF-50), primary forest (FOR) and pasture (PAS) in Eastern Amazon.

3.5. Influence of AFS succession on soil enzyme activity

Across the land uses, the transition from degraded pastures to long-term agroforests enhanced the activity of β-glucosidase, arylsulfatase, and acid phosphatase ($p < 0.001$). Especially in the top 0-10 and middle 10-20 cm layers (Figure 13). All three enzymes activity rapidly increased at the 0-10 cm layer, with β-glucosidase rapidly increasing in AF-7 (126.7%), AF-35 (59.82%), AF-50 (162.5%) and FOR (14.96%) sites when compared with the previous stage (Figure 13A).

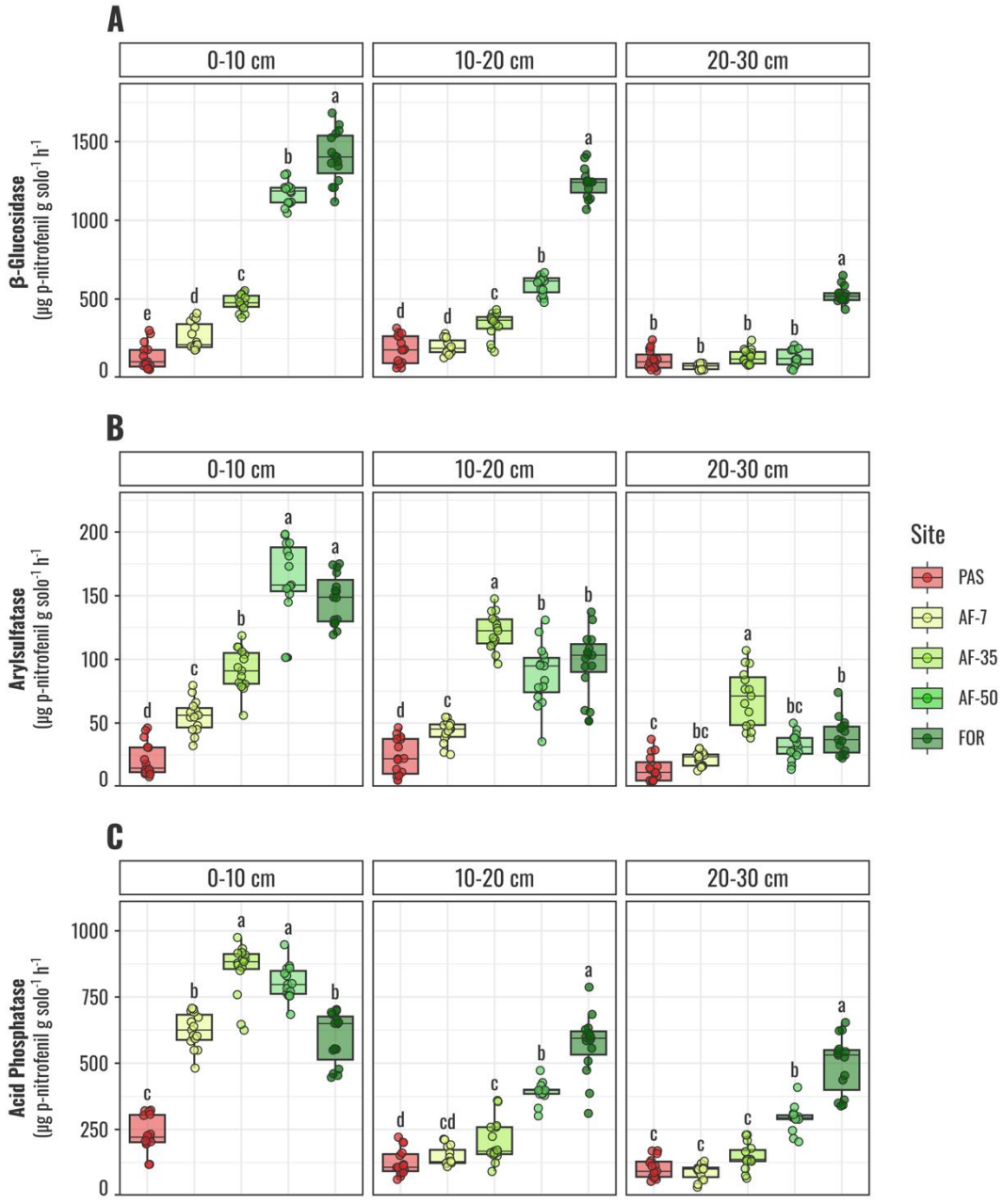

Figure 13. Soil enzyme activities across land use and depths Soil enzyme activities across land use and depths. β-glucosidase (A), arylsulfatase (B), and acid phosphatase (C) in three depth intervals (0–10, 10–20, and 20–30 cm) under five land-use systems: pasture (PAS), 7 years old AFS (AF-7), 35 years old AFS (AF-35;), 50 years old AFS (AF-50) and native forest (FOR).

Arylsulfatase and acid-phosphatase activity also increased in the soil surface with AFS age, as the AF-50 arylsulfatase activity reached 162.9 µg p-nitrophenol $g^{-1}h^{-1}$, which was statistically the same as the native forest activity (Figure 13B). The same could also be observed for acid-phosphatase activity, with AF-35 and AF-50 reaching similar values to FOR in

the 0-10 cm layer (Figure 13C). In the deeper 10-20 and 20-30 cm soil layers, overall enzyme activity decreased compared to the 0-10 cm layer. Although AFS significantly enhanced all three enzyme activities to a lesser degree, the land-use effects began to dilute with soil depth.

3.6. Bacterial and fungal abundance

The abundance of the bacterial and fungal communities was assessed through qPCR assay of the 16S rRNA and ITS regions. The qPCR assays presented R^2 values between 0.95 and 0.98 and efficiency between 80 and 95% based on the regression line of each fragment standard curve. Mean log_{10}-ITS abundance significantly increased with the land use succession from degraded pasture to agroforests and then forests (Figure 14A).

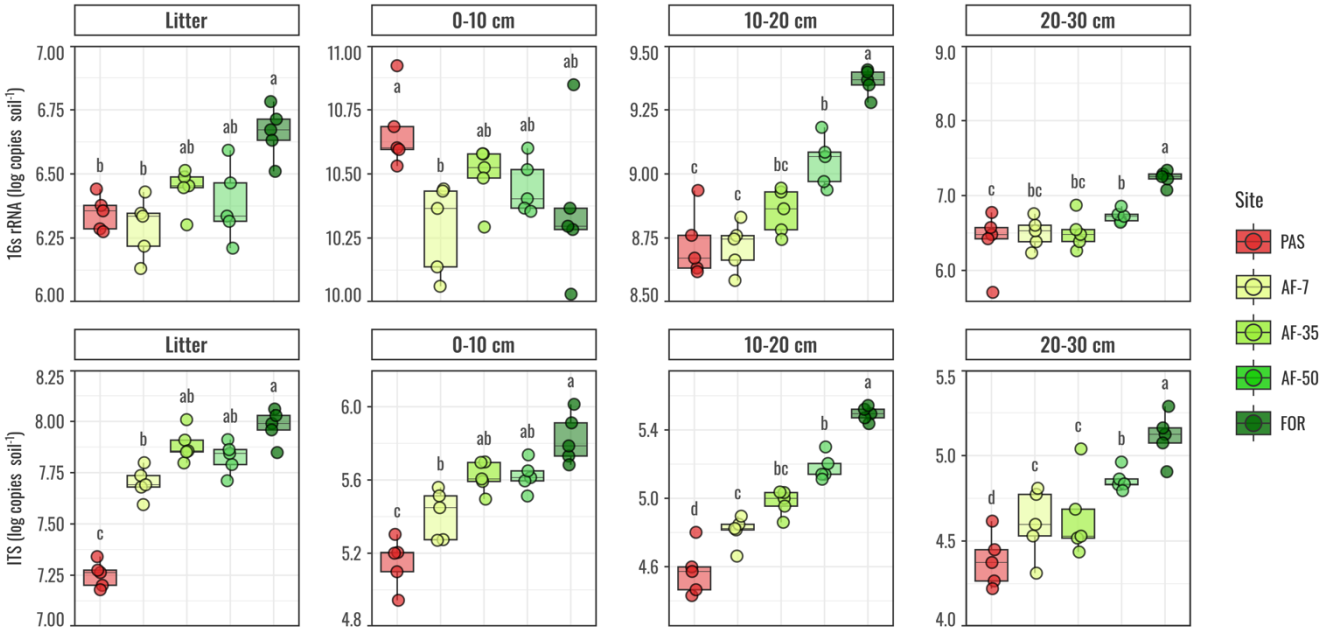

Figure 14. Boxplots show log_{10} of the 16S rRNA (bacterial) and log_{10} ITS (fungal) gene copy numbers across the litter layer and three soil depths (0–10, 10–20, 20–30 cm) for degraded pasture (PAS), 7-years (AF-7), 35-years (AF-35), 50-years (AF-50) agroforests and primary forest (FOR). Different letters denote significant differences (Dunn's test, $p < 0.05$) within each panel.

Fungal abundance was higher in the litter than in any soil layer, ranging from 7.25 in the PAS to 7.98 in the FOR site. The soil ITS abundance followed the same trend as the litter (Figure 14A). In contrast, the 16S rRNA response was mixed and different by each analyzed matrix (Figure 14B). The highest bacteria abundance in the litter layer was 6.66 in the FOR site. In contrast, 16S rRNA abundance was higher in the 0-10 cm layer than in litter, with the

highest values found in PAS. This trend with land use succession was reversed in the 10-20 and 20-30 cm layers, gradually increasing from PAS to FOR sites.

3.7. Effects of land use succession on litter-associated bacterial and fungal assembly

A total of 15,859 Bacteria and 8,434 Fungi ASVs were identified at a 99% sequence similarity index. Taxonomic classification of the Bacteria at the phylum level showed that samples were mainly dominated by Proteobacteria and Firmicutes (Figure 15A). Proteobacteria presented lower overall dominance over the total bacterial abundance in PAS sites, with other phyla like Bacteroidota and Actinobacteriota also occupying a relevant part of the total community. As land use succession progressed, the dominance of Proteobacteria increased till almost total dominance in FOR sites. The phylum-level classification of the Fungi community was dominated by Ascomycota (Figure 15B). As land use succession progressed, Basidiomycota, Mortierellomycota, and Rozellomycota gained space in the fungal community of AF-50 and FOR sites. Bacterial Shannon diversity peaked in the AF-35 site, while both PAS and AF-7 had intermediate diversity, whereas AF-50 and FOR had the lowest bacterial diversity (Figure 16B). Fungal Shannon diversity did not differ between agroforests and forest sites, although all four were significantly higher than PAS fungal diversity (Figure 17B).

Bacterial and fungal genus biomarkers were identified across land uses (Figures 16A and 17A). Bacterial biomarkers showed that PAS was significantly enriched ($p < 0.05$) in Alphaproteobacteria such as *Sphingomonas*, *Chryseobacterium,* and *Mucilaginibacter*. AF-7 showed *Pseudorhizobium*, *Flavobacterium,* and *Nocardioides* as biomarkers, while *Pedobacter*, *Lysobacter,* and *Mesorhizobium* characterized AF-35. The AF-50 showed significant enrichment of *Raoultella, Burkholderia,* and *Klebsiella*. FOR featured *Weissella* and other Firmicutes as biomarkers. The analysis of the Fungi community assembly highlighted that members of *Fusarium, Pyrenochaetopsis*, *Paraconiothyrium,* and other *Dothideomycetes*–related genera were significantly enriched in the PAS sites, whereas AF-7 harbored a distinct assemblage of Basidiomycota such as *Letendraea* and *Lasionectria*. The mid-succession AF-35 was mainly characterized by higher relative abundances of *Amorocoelophoma* and *Plectosphaerella,* while in the late-succession AF-50, *Mortierella* and *Geastrum* emerged as discriminant taxa. Finally, the FOR site was distinguished by high enrichment of *Talaromyces, Trichoderma, Penicillium,* and *Acremonium*.

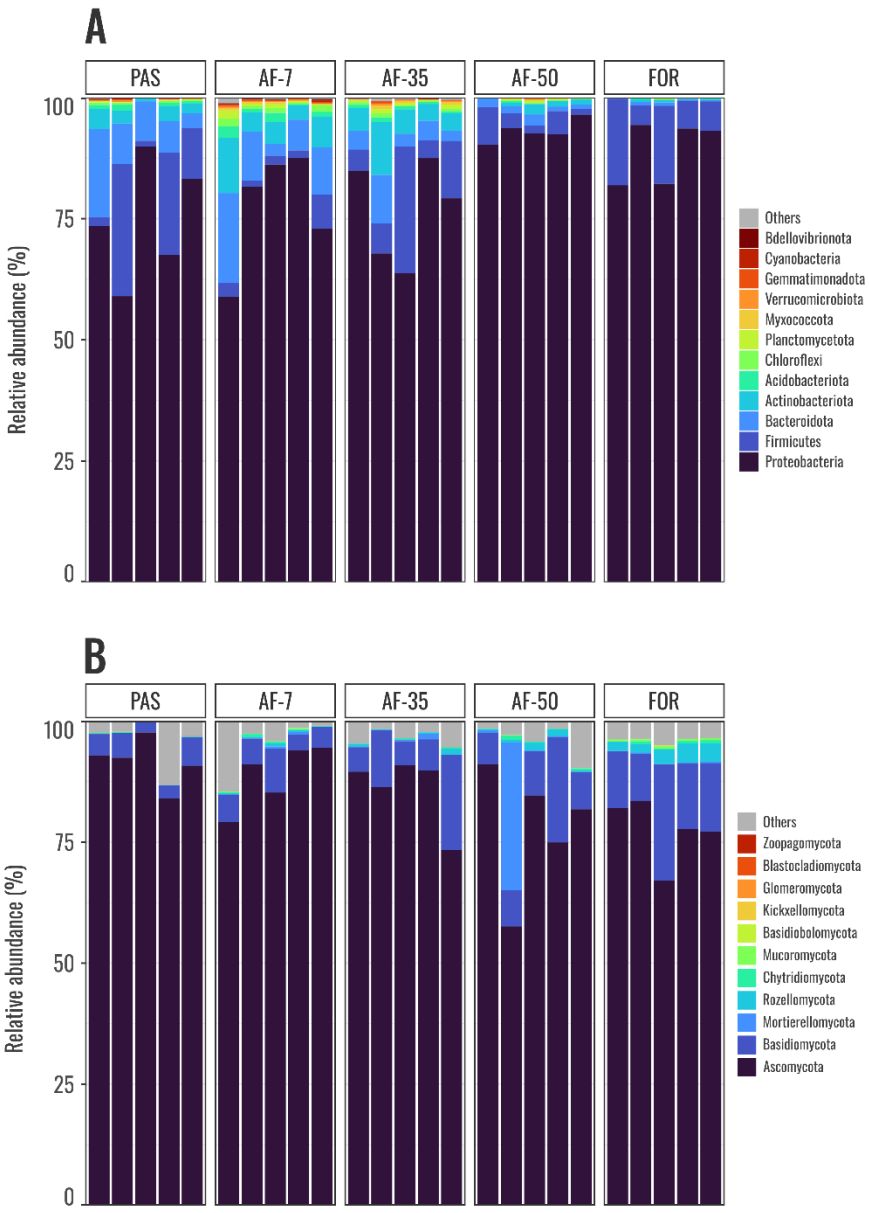

Figure 15. Bacterial and fungal microbial community composition in the litter layer in degraded pasture (PAS), 7-year (AF-7), 35-year (AF-35), 50-year (AF-50) agroforests, and primary forest (FOR).

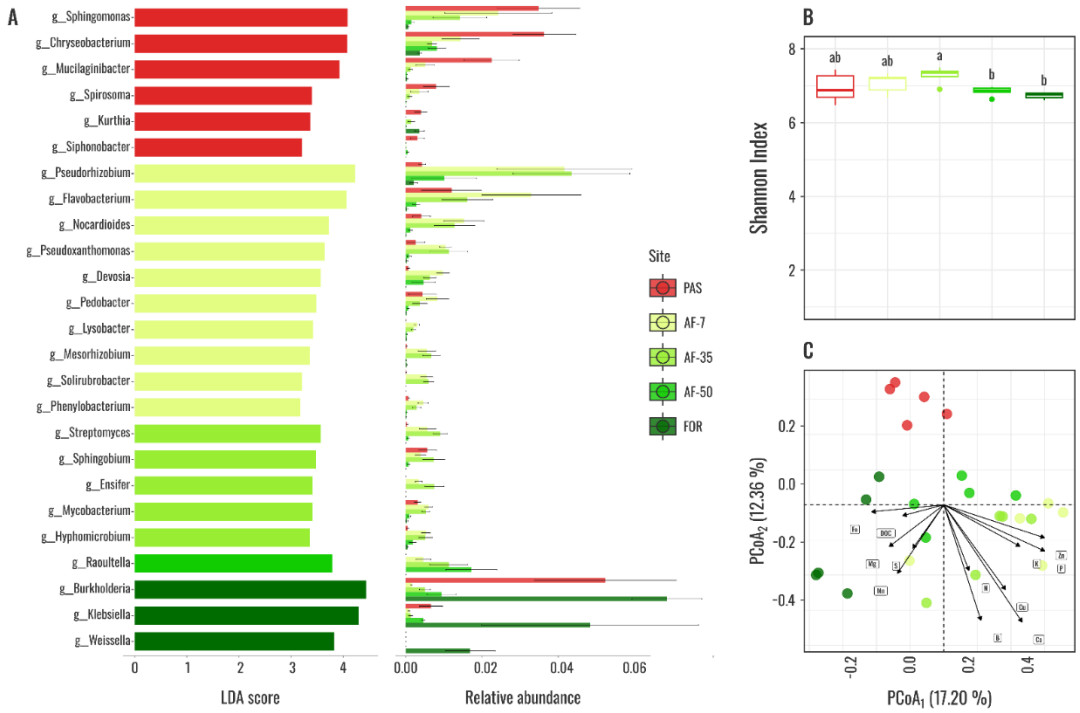

Figure 16. Successional shifts in bacterial communities. Successional shifts in bacterial communities. (A) Linear discriminant analysis (LDA) effect size (LEfSe) analysis of bacterial genera significantly enriched ($p < 0.05$) in degraded pasture (PAS), 7-year (AF-7), 35-year (AF-35), 50-year (AF-50) agroforests, and primary forest (FOR). (B) Shannon diversity (H′) of fungal communities (different letters denote Dunn's post-hoc at $p < 0.05$). (C) Principal coordinates analysis (PCoA) of Bray–Curtis dissimilarities. Overlaid vectors (envfit, $p < 0.05$) indicate the correlations of community composition with litter chemistry.

Table 7. Analysis of Similarities (ANOSIM) of the bacterial and fungal sequencing data of degraded pasture (PAS), 7-year (AF-7), 35-year (AF-35), 50-year (AF-50) agroforests, and primary forest (FOR)

Data	Land use	
	R^2	***p*-value**
Litter bacteria (16S rRNA)	0.3038	**< 0.001**
Litter fungi (ITS)	0.3827	**< 0.001**

Bold values indicate statistical significance at $p < 0.05$ (p-value). Distance indexes: Bray-Curtis (microbial communities). R^2: percentage of the variance explained. F: F-values.

Principal coordinates analysis (PCoA) based on the bacterial microbial community Bray-Curtis dissimilarity matrix (Figure 16C) revealed a significant dispersion pattern related to land use (Table 7). The first PCoA axis accounted for 17.2% of the observed dissimilarity, separating the primary forest from the agroforests. The second PCoA axis represented 12.4% of the observed variance and showed a clear separation of pasture from all other land uses. The environmental variables correlated with the bacterial community, showing that litter nutrients like P, K, Ca, B, Zn, Cu, and Mn explained bacterial dissimilarities (Table 8).

Table 8. Results of the envfit correlation analysis of the litter-associated bacterial and fungal community dissimilarity matrix with litter environmental variables for the pasture (PAS), 7-year (AF-7), 35-year (AF-35), and 50-year (AF-50) agroforests and primary forest (FOR) areas.

Nutrients	Bacteria		Fungi	
	R^2	p-value	R^2	p-value
Nitrogen (N)	0.1812	0.099 .	0.3727	0.004 **
Phosphorus (P)	0.4803	**0.001** ***	0.6622	**0.001** ***
Potassium (K)	0.2922	**0.004** **	0.1948	0.096 .
Calcium (Ca)	0.7403	**0.001** ***	0.7768	**0.001** ***
Magnesium (Mg)	0.1815	0.079 .	0.2017	0.083 .
Sulfur (S)	0.1071	0.287	0.0850	0.373
Iron (Fe)	0.2087	0.068 .	0.1243	0.244
Boron (B)	0.5384	**0.002** **	0.5261	**0.001** ***
Manganese (Mn)	0.2547	**0.040** *	0.3434	**0.012** *
Zinc (Zn)	0.4415	**0.002** **	0.5698	**0.001** ***
Cooper (Cu)	0.4113	**0.002** **	0.4468	**0.002** **
DOC	0.0711	0.445	0.2720	**0.028** *

C: Carbon (g kg^{-1}); DOC: Dissolved organic carbon (mg L-1); P: Phosphorus (g kg^{-1}); K: Potassium (g kg^{-1}); Ca: Calcium (g kg^{-1}); Mg: Magnesium (g kg^{-1}); S: Sulfur (g kg^{-1}); Fe: Iron (mg kg^{-1}); B: Boron (mg kg^{-1}); Mn: Manganese (mg kg^{-1}); Zn: Zinc (mg kg^{-1}); Cu: Cooper (mg kg^{-1}). Bold values indicate statistical significance at p-value < 0.05.

Fungal composition was significantly explained by land use changes (Table 7, Figure 17C). PAS fungal composition was highly dissimilar to other land uses, clustering afar from them, while AF-7 and AF-35 were closely clustered. AF-50 clustered separately from other agroforests, being closest to FOR. The envfit analysis correlated the nutrients such as P, Ca, B, Mn, Zn, Cu, and the litter DOC to the microbial community. Interestingly, the litter DOC had a significative impact on the fungal composition, showing a higher correlation with the AF-50 and FOR sites.

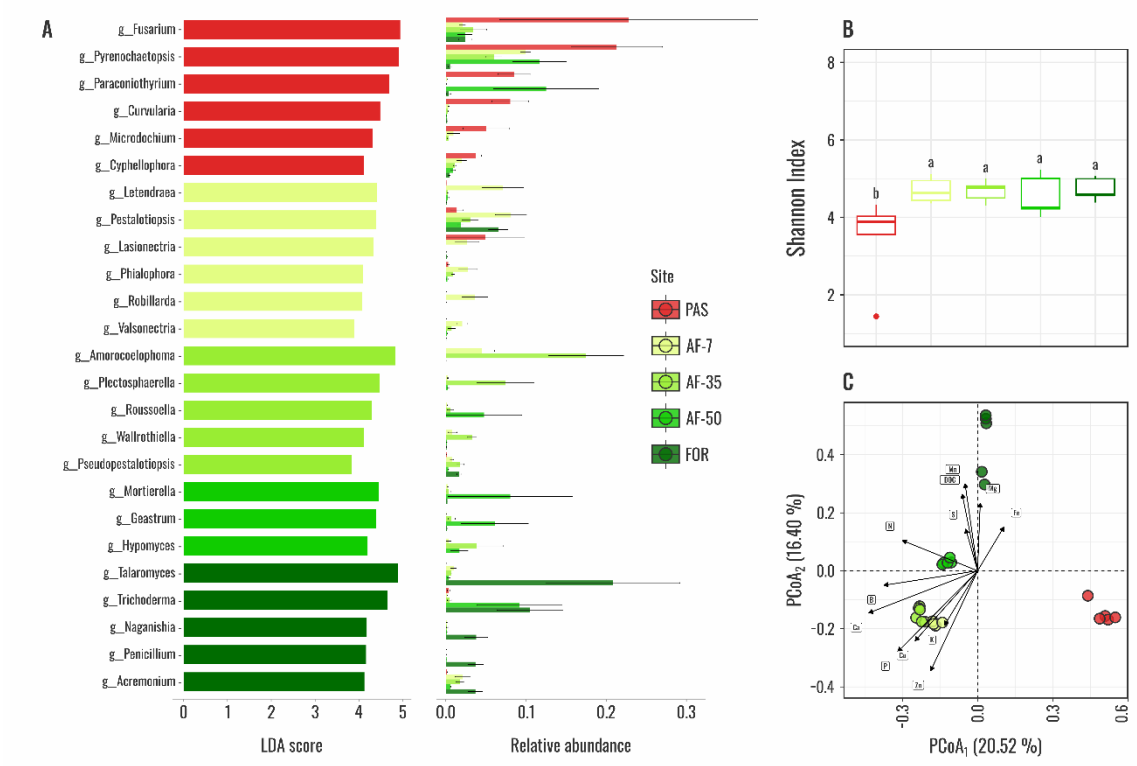

Figure 17. Successional shifts in litter fungal communities. (A) Linear discriminant analysis (LDA) effect size (LEfSe) analysis of fungal genera significantly enriched ($p < 0.05$) in degraded pasture (PAS), 7-year (AF-7), 35-year (AF-35), 50-year (AF-50) agroforests, and primary forest (FOR). **(B)** Shannon diversity (H′) of fungal communities (different letters denote Dunn's post-hoc at $p < 0.05$). **(C)** Principal coordinates analysis (PCoA) of Bray–Curtis dissimilarities. Overlaid vectors (envfit, $p < 0.05$) indicate the correlations of community composition with litter chemistry.

3.8. Effects of land use succession on soil bacterial and fungal assembly

The bacterial community at the phylum level showed that Proteobacteria and Firmicutes were the most abundant phyla across sites (Figure 18). However, the dominance of the two phyla was less pronounced than in the litter layer, leaving space for other phyla like Actinobacteria, Bacteroidota, Firmicutes, Verrucomicrobiota, and Chloroflexi. As land use succession progressed, Proteobacteria members progressively increased relative abundance, representing almost half of the community in AF-50 and FOR. Ascomycota members heavily dominated the soil fungal community at the phylum level (Figure 18). However, as with the succession of land uses, other phylum like Basidiomycota, Mortierellomycota, and Chytridiomycota increased their relative abundance, resulting in a relative suppression of ascomycetes.

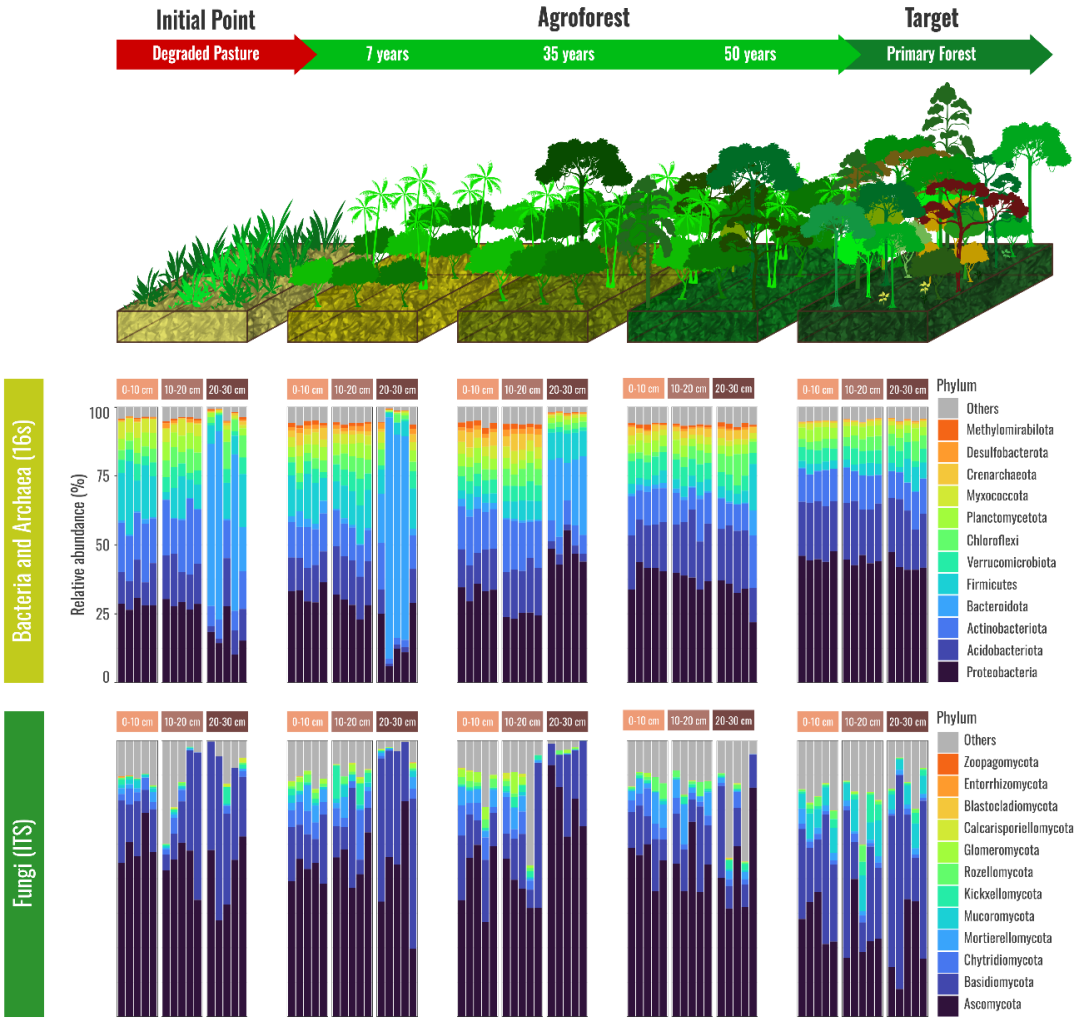

Figure 18. Bacterial and fungal microbial community composition in the soil across three depth intervals (0–10, 10–20 and 20–30 cm) under five land use systems: pasture (PAS), 7 years old AFS (AF-7), 35 years old AFS (AF-35), 50 years old AFS (AF-50) and native forest (FOR).

The microbial alpha diversity showed significant differences across sites, especially at deeper soil layers (Figure 19). The Shannon index showed that bacterial diversity in the surface layer (0-10 cm) was the highest in AF-50 and the lowest in AF-7, with no significant differences among other sites. At the same time, the deepest soil layer (20-30 cm) showed the lowest alpha diversity for AF-7 and the highest at FOR. The fungal diversity did not significantly differ on the surface, but AF-50 showed the highest alpha diversity in the second and third soil layers.

Figure 19. Shannon diversity index of (A) bacterial community and (B) fungal community. Each panel's lowercase letters denote significant pairwise differences (Dunn's test, $p < 0.05$).

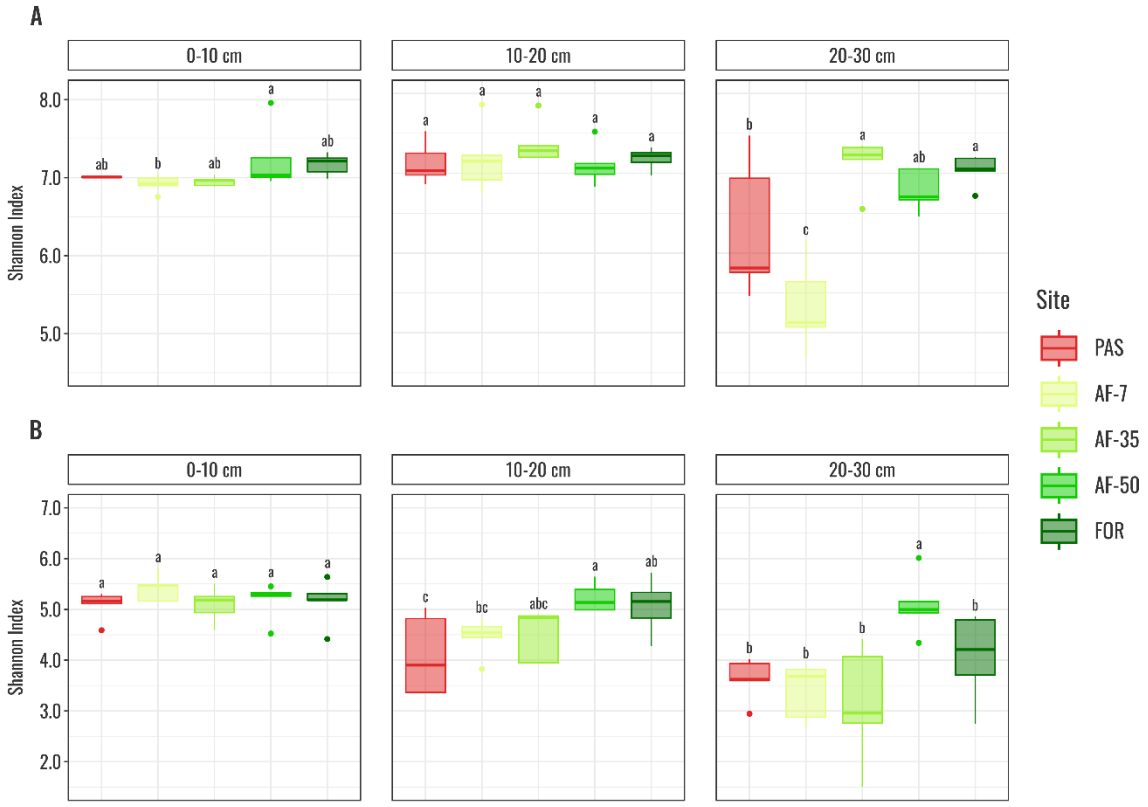

Table 9. Analysis of Similarities (ANOSIM) of the soil bacterial and fungal sequencing data of degraded pasture (PAS), 7-years (AF-7), 35-years (AF-35), 50-years (AF-50) agroforests and primary forest (FOR)

Data	Land use		Soil Layers	
	R2	P-value	R2	P-value
Soil Bacterial Community	0.4166	< 0.001	0.3054	< 0.001
Soil Fungal Community	0.6466	< 0.001	0.1735	< 0.001

Similar to the chemical profile and microbial litter community composition, we used the non-parametric Analysis of Similarity (ANOSIM) and confirmed the significance of observed trends between the total bacterial and fungal communities across land uses displayed at the NMDS plots (Figure 20, Table 9). The bacterial community significantly responded to changes in land use ($R^2 = 0.41$, $p < 0.001$) and in soil depth ($R^2 = 0.30$, $p < 0.001$) to almost the same degree (Table 9). In contrast, the fungal community was far more responsive to land use

(R^2 = 0.64, $p < 0.001$) than to soil depth (R^2 = 0.17, $p < 0.001$). The AF-50 and FOR bacterial and fungal communities consistently clustered across the soil profile, while PAS, AF-7, and AF-35 clustered separately, as they were more similar at the soil surface and more dissimilar as depth increased (Figure 20).

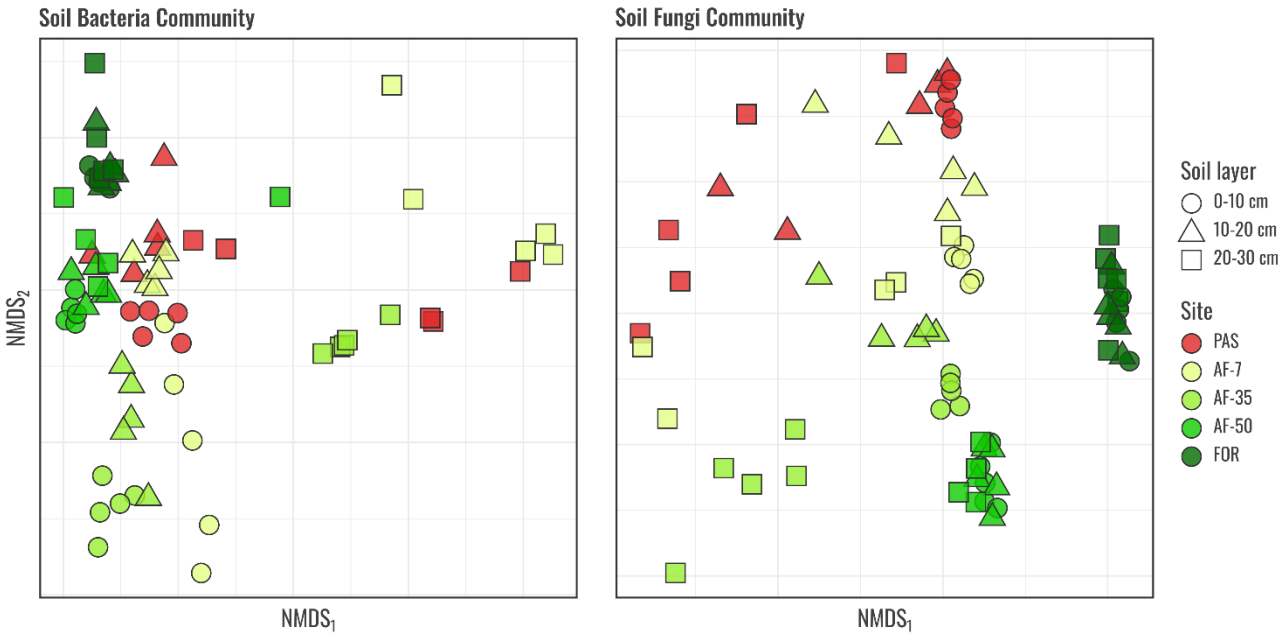

Figure 20. NMDS based on Bray-Curtis dissimilarity of soil bacterial and fungal communities. Site abbreviations: degraded pasture (PAS), 7-year (AF-7), 35-year (AF-35), 50-year (AF-50) agroforests, and primary forest (FOR).

Environmental variables were also significantly correlated with both microbial domains (Table 10). For bacteria, the relevant soil chemical attributes were soil pH (R^2 = 0.49), exchangeable Ca (R^2 = 0.59), Mg (R^2 = 0.648), available P (R^2 = 0.44), Zn (R^2 = 0.45), Al^{3+} (R^2 = 0.60), and DOM (R^2 = 0.38). For the fungal community, variables like C-MAOM (R^2 =48), C-DOM (R^2 = 0.47), β-glucosidase (R^2 = 0.51) and acid phosphatase activities (R^2 = 0.46) were strong predictors of the observed changes.

Table 10. Results of envfit correlation analysis of the soil bacterial and fungal community dissimilarity matrix with litter environmental variables for the pasture (PAS), 7-years (AF-7), 35-years (AF-35), 50-years (AF-50) agroforests and primary forest (FOR) areas.

Soil attributes	Bacteria		Fungi	
	R^2	p-value	R^2	p-value
pH	0.4981	**0.001** ***	0.1146	**0.014** *
C-SOM	0.0135	0.616	0.1497	**0.006** **
C-POM	0.2124	**0.001** ***	0.3035	**0.001** ***
C-MAOM	0.2028	**0.002** **	0.4811	**0.001** ***
C-DOM	0.3853	**0.001** ***	0.4769	**0.001** ***
N	0.0127	0.629	0.1612	**0.004** **
P	0.4446	**0.001** ***	0.1079	**0.015** *
K	0.2141	**0.001** **	0.0136	0.630
Ca	0.5985	**0.001** ***	0.0474	0.173
Mg	0.6480	**0.001** ***	0.0775	0.064 .
S	0.0345	0.289	0.2115	**0.001** ***
Al	0.6015	**0.001** ***	0.3533	**0.001** ***
B	0.2140	**0.002** **	0.0307	0.318
Cu	0.3319	**0.001** ***	0.3539	**0.001** ***
Fe	0.2406	**0.001** **	0.3206	**0.001** ***
Mn	0.3231	**0.001** **	0.1199	**0.009** **
Zn	0.4556	**0.001** ***	0.0116	0.659
Density	0.1928	**0.002** **	0.3451	**0.001** ***
β-glucosidase	0.3147	**0.001** ***	0.5151	**0.001** ***
Arylsulphatase	0.2259	**0.001** **	0.3884	**0.001** ***
Acid phosphatase	0.3303	**0.001** ***	0.4642	**0.001** ***

Bold values indicate statistical significance at p-value < 0.05.

3.9. Depth-stratified soil bacterial and fungal indicator taxa across a land-use successional gradient

Bacterial and fungal genus biomarkers were identified across land uses and soil layers, revealing depth-stratified patterns (Supplementary Tables 4–9). Across the surface layer (0-10 cm), PAS soils were dominated by spore-forming *Bacillus* and *Lysinibacillus*, together with *Conexibacter* and *Haliangium*, alongside the Ascomycetes *Sodiomyces* and *Penicillium*, and the basidiomycete *Clitocybe*. In AF-7, bacterial biomarkers like *Pedomicrobium* and *Nordella* paired with *Tumebacillus* and *Luedemannella* were identified, with their corresponding fungal indicators like *Fusarium* and *Psathyrella*. After 35 years, in AF-35 sites, soil biomarkers were *Gaiella*, *Nitrospira*, and *Hyphomicrobium* (Proteobacteria), while fungal markers were mostly *Mortierella*, *Wallrothiella*, *Auxarthron*, and the arbuscular mycorrhizae *Pervetustus*. Fifty years of agroforestry cultivation further changed microbial biomarkers like

Pseudolabrys, *Candidatus Udaeobacter*, and *ADurb.Bin063-1*, along with *Roseiarcus* and *Anaerocolumna*, while the fungal markers were mostly ascomycetes like *Trichoderma*, *Clonostachys*, *Chloridium*, *Talaromyces*, and *Chaetosphaeria*. Forest soils exhibited the most taxonomic diversity among indicators, as indicated by the presence of *Acidibacter*, *Bradyrhizobium*, *Candidatus Koribacter*, *Acidothermus*, and *Candidatus Xiphinematobacter*. Fungal indicators comprised *Hygrocybe*, *Entoloma*, *Clitopilus*, *Scedosporium*, and *Melanconiella*.

Across the soil subsurface (10–30 cm), PAS soil microbial biomarkers remained characterized by bacterial and fungal genera like *Bacillus* and *Conexibacter*, *Sodiomyces*, and *Cladosporium*. The AF-7 was marked by microbial indicators such as *Ellin6067*, *Candidatus Nitrosotalea*, and the ascomycetes *Talaromyces* and *Scedosporium* in the 10–20 cm layer, while the deeper 20-30 layer was marked by *Mucilaginibacter*, *Methylobacterium*, *Paracamarosporium*, and *Schizophyllum* genera. By 35 years in AF-35, genera like *Gaiella* and *Nitrospira*, *Humicola*, and *Paracremonium* permeated the 10-20 cm layer, while the genera *Acinetobacter*, *Bacillus*, *Phomatospora*, and *Epicoccum* marked the 20-30 cm layer. After five decades of AFS, in the AF-50 site, the *Pseudolabrys*, *Auxarthron*, and *Trichoderma* were highlighted as strong markers of both 10-20 and 20-30 cm layers. In contrast, FOR soils had depth-persistent bacterial biomarkers such as *Acidibacter*, *Acidothermus*, *Candidatus Koribacter*, and *Bradyrhizobium*. Fungal biomarkers for the FOR site were more variable with depth, as genera such as Hygrocybe and *Peniophorella* marked the 10-20 cm layer, while *Dermoloma* and Scedosporium were selected as 20-30 cm biomarkers.

3.10. Soil health index (SHI) scores

The overall Soil Health Index (SHI) consistently increased with land use succession and declined with increasing depth (Figure 21). In the surface horizon (0–10 cm), SHI consistently increased in AF-7 (84.1%), AF-35 (47.3%), AF-50 (5.6%), and FOR (7.1%) sites when compared with the previous land use. In the 10-20 cm layer, we also observed the same trend as SHI consistently increased from PAS to AF-7 (57.9%), then to AF-35 (95.6%) and to AF-50 (0.19%), finally peaking in FOR (60.2%). In the last soil layer (20-30 cm), SHI was uniformly lower in PAS and AF-7, then increasing in AF-35 (139.4%) and slightly decreasing in AF-50 (-11.0%) to then increase again in FOR (62.8%).

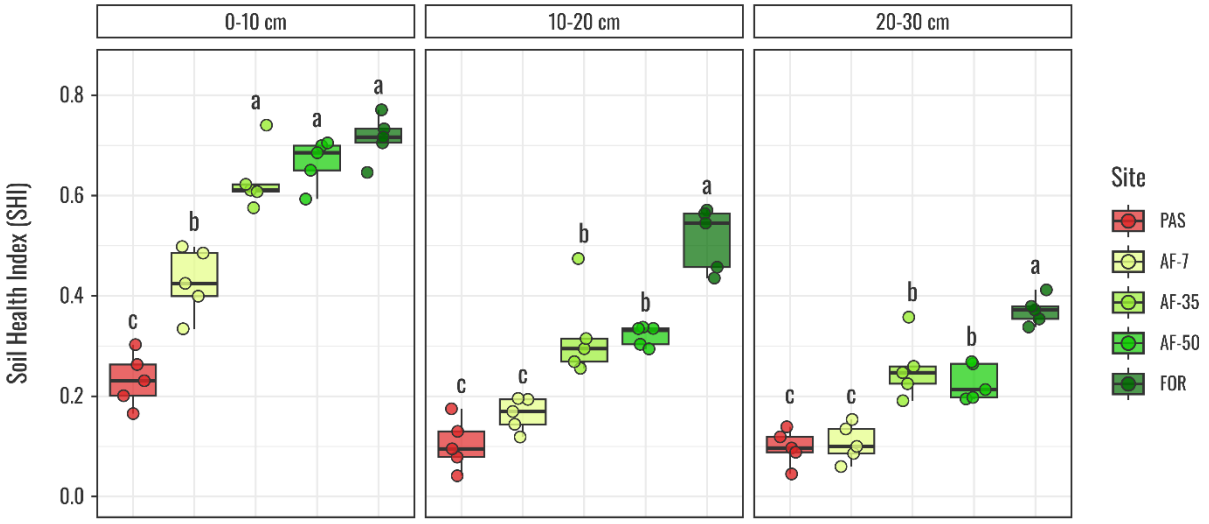

Figure 21. Overall soil health index (SHI) scores of degraded pasture (PAS), 7-years (AF-7), 35-years (AF-35), 50-years (AF-50) agroforests and primary forest (FOR) in the 0–10, 10–20 e 20–30 cm soil layers. Lowercase letters compare treatments for each sector (physical, chemical, and biological) through Dunn's test.

The Soil Health Index (SHI) revealed distinct successional trajectories across land uses and depths into physical, chemical, and biological sub-scores (Figure 22). In the soil surface, physical health (support root growth + water storage and aeration) increased from PAS through AF-7 (16.6%), AF-35 (10.3%) to AF-50 (27.7%) and FOR (8.5%). Chemical health (soil acidity regulation, nutrient availability, and nutrient storage) followed a similar but more pronounced pattern, rapidly rising from PAS to AF-7 (262.2%), to AF-35 (89.3%), then decreasing in AF-50 (-52.6%) and increasing again in FOR (17.22%). Biological health (energy for microbial activity, soil nutrient cycling, and habitat for microorganisms) was minimal in PAS and immediately increased in AF-7 (192.9%) to AF-35 (59.9%) and AF-50 (54.6%), which did not differ from FOR. Across the subsoil layers (10-20 and 20-30 cm), the physical health did not increase significantly from PAS to any AFS. Chemical health followed the same pattern as that observed on the soil surface, albeit to a lesser degree. Finally, biological health was minimal in both PAS and AF-7, steadily increasing in AF-35 and AF-50 till maximum values in FOR.

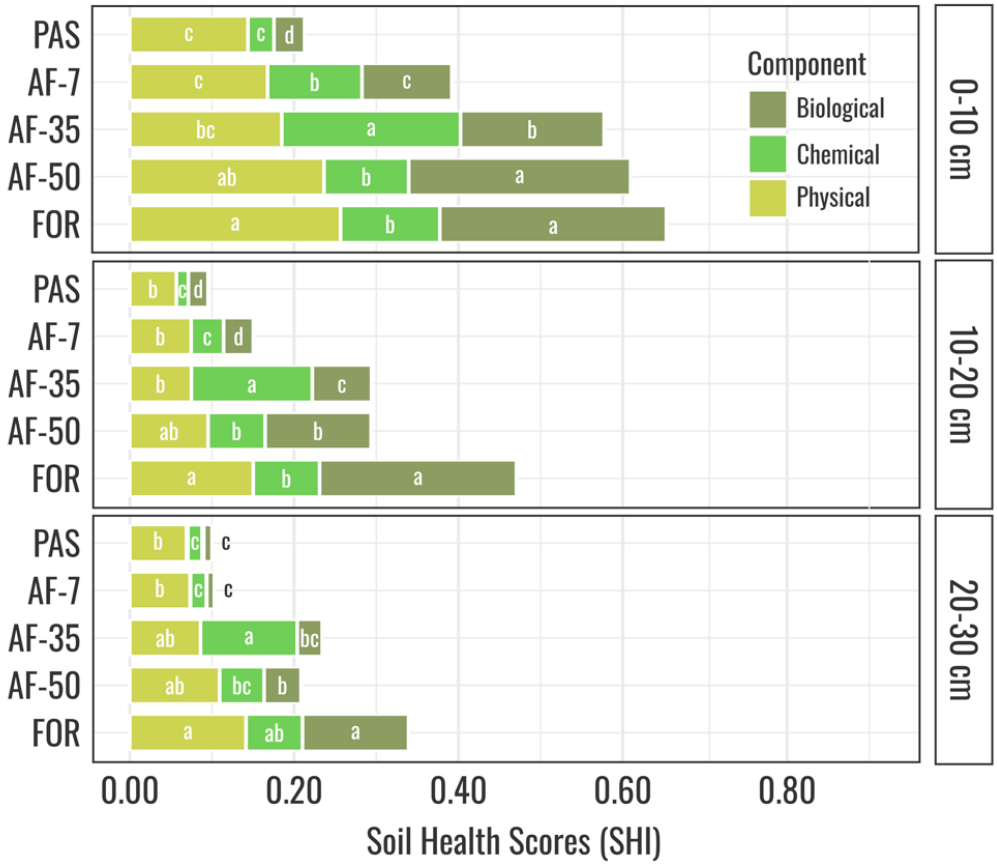

Figure 22. Contribution of physical, chemical, and biological component to the overall soil health index (SHI) scores under a degraded pasture (PAS), 7-year (AF-7), 35-year (AF-35), 50-year (AF-50) agroforests and primary forest (FOR) in the 0–10, 10–20 e 20–30 cm soil layers. Lowercase letters compare treatments for each component (physical, chemical, and biological) through Dunn's test.

4. DISCUSSION

4.1. AFS progression and recovery of ecosystem functions

Agroforests represent an alternative land use strategy for long-term agricultural production in the Amazon region, overcoming most of the environmental constraints that often make traditional agricultural practices unsustainable (Nair, 2014). Our study found that AFS succession (*i.e.,* the natural progression of these systems, as they are designed to last many years without heavy disturbances) from 7-50 years showed sequential increases in aboveground litter accumulation and litter carbon stocks, also enhancing litter quality as evidenced by its higher nutrient concentrations, reduced C/N ratio, and higher nutrient content. Compared to PAS, the litter layer gradually shifted from grass-like and nutrient-poor litter toward a more complex and nutrient-rich composition depending on the land use fertility management. These shifts in litter accumulation are likely a result of the gradual canopy closure (as captured by NDVI shifts) and aboveground tree biomass buildup that naturally occurs during AFS succession in Tomé-Açu (Batistella et al., 2013). These characteristics directly correlate with litter accumulation in rainforests and agroforests across the central Amazon (Martius et al., 2004).

Changes in the litter isotopic composition ($\delta^{13}C$ and $\delta^{15}N$) further solidify the role of AFS in litter quality changes, as the observed changes in litter $\delta^{13}C$ are most likely a result of the shift from mixed C_4-C_3 carbon derived from grasses and herbaceous plants in the PAS site to mostly C_3 carbon derived from trees (de Oliveira et al., 2022; Martinelli et al., 2009). Oppositely, the lowers values of $\delta^{15}N$ observed in the PAS and AF-7 and AF-35 litter may result from external N inputs, as atmospheric N_2 fixated into ammonia through the Haber-Bosh process (Martinelli et al., 2009). In contrast, the ^{15}N enrichment in AF-50 and FOR sites is likely due to increases in litter decomposition and enhanced nutrient cycling, as the lighter ^{14}N is more easily absorbed and metabolized by plants and microorganisms (Broadbent et al., 2014; Riggs et al., 2015). AF-50 and FOR litter layers also had considerably higher DOC concentrations, further suggesting higher decomposition rates due to microbial activity, as large amounts of the litter mass are leached as dissolved organic matter (DOM) during microbial decomposition (Soong et al., 2015).

AFS also presented considerable increases carbon stocks across both the POM and MAOM fractions of SOM. This gradual formation of SOM from the topsoil to the bottom layers further indicates the role of aboveground C inputs and belowground carbon fluxes (Powers; Marín-Spiotta, 2017). In fact, the observed enhancement in the POM fraction with the AFS

development stage can be associated with higher availability of plant residues in the litter layer, as plant-derived polymers are the primary contributor to POM formation in soils (Cotrufo et al., 2015). These observations also explain the nature of the elevated humification detected in the POM fraction by laser-induced fluorescence spectroscopy, as the observed fluorescence spectra are mainly derived from the excitement of aromatic and alkyl structures derived from plant structural polymers (Milori et al., 2006, 2002). At the same time, AFS development also significantly enhanced MAOM formation at the soil surface, which is mainly derived from low molecular weight, soluble organic compounds from the DOM (Cotrufo; Lavallée, 2022). Particularly high concentrations of DOC were observed in the litter and 0–10 cm layers of the AF-50 and FOR sites, which were consistent with higher MAOM stocks and indicate that AFS promotes SOM stabilization. We find ourselves in agreement with Gmach et al. (2020), who reported that DOM derived from aboveground residues is expected to contribute to the formation of SOM in the topsoil, while DOM derived from exudates and root litter decomposition would contribute to SOM formation at deeper layers.

We also observed considerable increases in bulk SOM C and N content as AFS developed, which were especially evident at the soil surface layer (0-10 cm) and gradually diluted as soil depth increased. Both PAS and AF-7 did not differ in C and N contents, in line with what Cardozo et al. (2022) observed when evaluating SOC changes after AFS establishment, which were only able to find SOC increments after 8 years. Significant increases in C and N contents and SOC stocks were observed in AF-35- and AF-50 AFS sites. At this stage, AFS in the Amazon display a relatively closed canopy and can develop structures similar to secondary forests as they age, recovering C stocks at the same rate or faster than secondary forests (Cardozo et al., 2022). Further insights into the SOM dynamics were provided by stable isotope ratio analysis of the soil $\delta^{13}C$ and $\delta^{15}N$. PAS SOM and the POM and MAOM fractions $\delta^{13}C$ presented the classical signature of C derived from mixed C_4 and C_3 sources, typical of degraded pastures due to the presence of broadleaf weeds (de Oliveira et al., 2022). Interestingly, when comparing both POM and MAOM fractions in the PAS site, we observed higher enrichment in ^{13}C across the MAOM, suggesting higher contribution of grass-C to this fraction formation, as the majority of C inputs in grasslands and pastures are derived from root exudation (Mitchell et al., 2021), and are more prone to contribute to the formation of MAOM according to the microbial efficiency matrix stabilization (MEMS) framework proposed by Cotrufo et al. (2015). As AFS develops, the $\delta^{13}C$ gradually decreases as the constant C inputs from C_3 trees gradually take over most SOM pools. Also, it is worth noting that both $\delta^{13}C$ and

$\delta^{15}N$ were progressively higher in deeper soil layers, likely due to isotopic fractionation of both ^{13}C and ^{15}N as the soil organic matter decomposes. As soil microorganisms decompose SOM and its fractions, the lighter C isotope (^{12}C) is more easily lost as CO_2. In comparison, the lighter N isotope (^{14}N) is preferably absorbed by plants or lost as N_2O during nitrification and denitrification, enriching the soil in its heavier counterparts in deeper layers (Bieluczyk et al., 2023; Martinelli et al., 2009).

4.2. Agroforest succession increased microbial activity and abundance in a depth-stratified pattern

Overall, the progression of land use from PAS to AF-7, AF-35, and AF-50 enhanced the potential activity of β-glucosidase, arylsulfatase, and acid phosphatase across the 0-10, 10-20, and 20-30 soil layers. Bacterial and fungal abundance also increased across land use succession, mirroring the top-to-bottom pattern of extracellular enzymes. These findings reinforce the joint adoption of enzymatic and molecular assays as sensitive indicators of the impacts of land use changes on microbial activity across croplands(Carneiro et al., 2024; Lopes et al., 2018, 2013). These shifts were not homogeneous but primarily increased alongside land use succession, peaking in more developed systems with greater labile carbon availability (AF-35, AF-50, and FOR). The relationship between soil carbon pools and soil enzymatic activity has long been established (Lopes et al., 2013), and the observed gradual recovery of SOM across its fractions can be linked to enhanced tree cover and carbon inputs in AFS (Castro et al., 2024). These processes can ultimately lead to increased energy availability and the observed rise in microbial enzymatic activity.

4.3. AFS exhibit divergent microbial communities as they develop

The analysis of the bacterial taxonomic composition of the litter and soil matrices revealed increasing relative abundance of the phyla Proteobacteria and Firmicutes as land use succession progressed, which dominated most of the microbial community at this taxonomic level in FOR sites. The inverse trend was observed for the fungal taxonomic composition, as Ascomycota's relative abundance decreased, and other phyla like Basidiomycota, Mortierellomycota, and Chytridiomycota were able to increase their share of the total community. These trends were observable at one of the lowest taxonomical resolutions and followed previous research in oil palm-based AFS in Eastern Amazon (Rocha, 2024). This behavior is usually seen in the Amazon, as forest-to-pasture conversion can decrease the abundance of many Proteobacteria microorganisms due to increased niche availability (Navarrete et al., 2013; Pedrinho et al., 2023). These shifts in the fungal community can also

be attributed to the increasing vegetation cover and litter inputs, which can favor wood-decomposing fungi (Cutler et al., 2014). In contrast, pastures usually favor more generalist fungi adapted to environmental shifts and dissimilar inputs (Mueller et al., 2016).

Microbial community diversity indicated by Shannon's H' index varied across land uses in both litter and soil layers. However, the effects of AFS establishment in the litter and soil surface layers were mainly observed in the bacterial H', while fungal H' remained consistent across AFS and FOR sites. More profound changes occurred in the soil subsurface layers, as both bacteria and fungi Shannon's H' index increased in long-term AFS (AF-35 and AF-50) and FOR sites. These shifts are likely fueled by gradual changes in aboveground C inputs and carbon buildup across SOM pools, especially as DOM (Gmach et al., 2020). These organic molecules are constantly leached from plant litter and SOM degradation, seeping through the soil profile and fueling changes in the soil microbiome assembly (Benk et al., 2019; Kallenbach et al., 2016; Roth et al., 2019).

During its passage through the soil layers, these organic molecules can be immobilized onto the surface of mineral particles and selectively metabolized by microorganisms (Kaiser; Kalbitz, 2012; Roth et al., 2019). These interactions between aboveground soluble inputs and microorganisms are also thought to be one of the primary contributors to SOM buildup in the MAOM fractions, as previously observed in AF-50 and FOR sites. Previous studies on Amazon soils also observed similar trends (Mendes et al., 2015a, 2015b; Navarrete et al., 2015). However, our measurements are derived from microbial amplicon sequencing and are inherently taxonomical and not functional. Thus, this increase in diversity can also indicate an increase in ecosystem resilience in AFS, as increasing diversity often leads to an increase in functional diversity and functional redundancy, increasing the system's ability to overcome environmental constraints and disturbances (Mendes et al., 2015a; Pedrinho et al., 2023).

Their beta diversity also highlighted further distinctions between the microbial communities across land uses, revealing interesting patterns. FOR and AF-50 bacterial and fungal communities were tightly clustered across the litter and soil layers. Beta diversity was measured through a Bray-Curtis dissimilarity matrix, meaning that the proximity between points reflects the enhanced similarity between their microbial community composition, indicating lower disturbance levels and enhanced regeneration of soil characteristics in AF-50. When evaluating the dynamics of both bacterial and fungal communities in Eastern Amazon AFS, Leite et al. (2023) found that AFS favored bacteria, while the natural regeneration of Amazon forests slowly shifted towards fungi. However, in our analysis, older AFS consistently

shifted biological, chemical, and physical characteristics toward those found in native forests. In this scenario and under this specific management, we argue that after 50 years, AFS was able to shift its communities toward a more forest-like one.

Typical to many studies (Buckeridge et al., 2020; Mendes et al., 2015a; Navarrete et al., 2013), soil chemical components like pH, Ca, Mg, P, Mn, Zn, and Al were the most important drivers of the dissimilarities observed in the bacterial community alongside physical components like bulk density and biological factors such as β-glucosidase acid phosphatase activities. Soil chemistry also played a significant role in the observed dissimilarities of the fungal community, with elements like S, Fe, and Cu able to explain a significant portion of the dissimilarities. However, physical and biological components such as bulk density, β-glucosidase, and acid phosphatase activities were able to explain more of the fungal observed dissimilarity. The importance of pH is inherently explained by its chemical properties, as the potential of hydrogen in soil (*i.e.*, the activity of H^+ ions in the soil solution) determines the availability of many nutrients and toxic ions in the soil solution. At the low pHs observed in PAS, AF-7, and AF-35, the solubility of Fe, Mn, Zn, and Cu ions gradually increases as metal hydroxides are solubilized into the soil solution (Sparks et al., 2024), becoming toxic to many organisms and partially explaining their importance in microbial community dissimilarities. In commercial AFS, the acidity correction through soil liming introduces large quantities of calcium carbonates ($CaCO_3$) or calcium-magnesium carbonates ($CaMg(CO_3)_2$) which then react with soil water, Al^3 and H^+ ions, neutralizing the acidic pH and immobilizing Al^3 and other toxic ions into their mineral forms, while also freeing Ca^{2+} and Mg^{2+} in the process (Sparks et al., 2024). Only the bacterial communities responded to Ca and Mg, further amplifying the role of these ions as key drivers of bacterial community dissimilarity in the Amazon following observations made by Navarrete et al. (2013). Physical and biological factors also were important drivers of microbial community dissimilarity. Variables like soil enzymatic activity and carbon stocks are often associated with land use changes, and the observed changes and their influence on microbial community changes can be pointed out as a result of increasing energy sources for microbial activity (Navarrete et al., 2015, 2013).

The differential abundance analysis of bacterial and fungal genera across the distinct land uses and soil layers indicated enriched genera for each site. In degraded pastures, temperature and water availability can shift dramatically compared to less disturbed agroecosystems, while organic inputs become scarcer and more recalcitrant (Müller et al., 2004). Under these conditions, the enrichments in genera affiliated to Firmicutes such as

Bacillus, *Lysinibacillus*, *Tumebacillus*, and Actinobacteriota like *Conexibacter* suggest a shift towards traits like tolerance to environmental shifts, metabolic versatility, and stress resistance (Battistuzzi; Hedges, 2009; Rodrigues et al., 2013). Members of these genera are commonly found in soils subjected to extreme daily temperatures and low moisture conditions (Lacerda-Júnior et al., 2019), characteristics usually found in degraded pastures.

Across AFS successional stages (AF-7, AF-35, AF-50), we observed a shift from disturbance-adapted microbial community assembly towards a community characteristic of less disturbed environments, resembling the native forest assembly in many ways. In early-stage AFS, surface horizons were dominated by spore-forming Firmicutes alongside fast-growing saprotrophic Ascomycota and Basidiomycota. The persistence of taxa with stress-resistant traits (*e.g.*, spore formation) are consistent with microbial shifts observed after land use changes and disturbances (Philippot et al., 2021), while the proliferation of opportunistic decomposers is likely linked to newly available C inputs from young cacao (*Theobroma cacao* L.) and açaí (*Euterpe oleracea* Mart.) trees similar to what occurs in early secondary succession (Powers and Marín-Spiotta, 2017). By 35 years (AF-35), enriched taxa were mainly chemolithoautotrophic containing genera such as ammonia-oxidizing archaea (*e.g.*, *Ca. Nitrosotalea*) and nitrite-oxidizing bacteria like *Nitrospira*, indicating a shift toward enhanced nitrogen cycling and complex substrate degradation (Koch et al., 2019; Lehtovirta-Morley et al., 2024). The rise of fungal saprotrophs such as *Humicola*, *Paracremonium*, *Hansfordia*, and *Mortierellomycota* also indicates enhanced decomposition of complex SOM in deeper layers, as some of them have also been previously linked to complex SOM degradation in the highly complex Amazon dark earth soils (Lucheta et al., 2016). At the same time, the presence of Glomeromycota (*Pervetustus*) suggests the presence of mycorrhizal networks that may facilitate deeper nutrient acquisition (El Hilali et al., 2022).

At AF-50, the microbial community closely resembles that of undisturbed forest soils. Surface layers are dominated by oligotrophic Verrucomicrobiota (*Ca. Udaeobacter*) and specialist saprotrophs (*Clonostachys*, *Trichoderma*), reflecting stable C inputs in late stages of succession (Banning et al., 2011; Liang et al., 2021). Mid-profile and deep horizons remain enriched in chemolithoautotrophs (*Pseudolabrys*, *Pedomicrobium*) and Actinobacteriota (*Streptomyces*), while the reappearance of the fruiting wood-decaying Basidiomycota (*Grammothele*, *Geastrum*) at deeper layers further underscores the availability of complex substrates in deeper layer and the importance of lower disturbances to the long-term buildup of SOM throughout the soil profile (Chaopricha; Marín-Spiotta, 2014; Lorenz; Lal, 2005).

4.4. Soil Health Index as an integrative indicator of succession

Our findings showed that Amazon AFS progressively increases litter and soil C stocks in the particulate organic matter (POM) and mineral-associated organic matter (MAOM) fractions, positively impacting soil biological activity (as indicated by higher diversity, abundance, and enzymatic activity), soil nutrient stocks (evidenced by increased nutrient availability and cation exchange capacity), and root growth (reduced soil bulk density). Additionally, our results jointly evidenced the maintenance and even regeneration of several ecosystem functions: (i) water storage and aeration, evidenced by reduced soil bulk density and balanced proportions between macro and microporosity; (ii) Soil acidity regulation and higher nutrient stocks, indicated by higher pH and nutrient availability; (iv) Nutrient storage, prompted by higher CEC; (v) Energy for microbial activity through enhance C availability throughout soil organic fractions; (vi) Soil nutrient cycling evidenced by soil enhanced enzymatic activity; (vii) Habitat for microorganisms a result of enhanced bacterial and fungal diversity and abundance. Integrating those findings into distinct soil health scores provided a multifunctional view of the contribution of physical, chemical, and biological characteristics, which revealed that AFS are not only able to enhance C storage in soils, but also recover multiple belowground ecosystem functions, corroborating previous studies (Bieluczyk et al., 2025b, 2025a; Naval et al., 2025).

5. CONCLUSION

Our findings demonstrate that cocoa-based agroforestry systems (AFS) on formerly degraded Amazonian pastures not only significantly enhance organic carbon storage across all SOM compartments (POM, MAOM, and bulk SOM) but also increased the soil health index at different compartments, such as physical, chemical, and biological soil properties, ultimately restoring multiple soil functions to levels approaching those of adjacent primary forests. Specifically, enhanced nutrient availability (evidenced by elevated stocks of P, K, Ca, and Mg) combined with improved pH buffering offered a more favorable chemical environment. At the same time, microbial activity and diversity were also markedly enhanced, as revealed by increased. qPCR-derived bacterial and fungal abundances and higher extracellular enzymatic activities of β-glucosidase, arylsulfatase, and acid phosphatase. These biological enhancements coincide with a clear shift in microbial community composition from pasture-dominated Ascomycota and Bacillus taxa to forest-associated Basidiomycota and Acidobacteriota, indicating the gradual reassembly of functionally diverse networks essential for carbon stabilization and nutrient cycling. Moreover, our data highlights the critical role of agroforests in restoring and maintaining C fluxes, especially through increased litter accumulation. ultimately resulting in the observed increases in SOM pools, microbial abundance, and diversity, which are components rarely investigated in the Amazon. Collectively, these results reinforce that well-managed cocoa-based AFS represent a viable long-term alternative to conventional agriculture in the Amazon, capable of restoring soil biological and chemical potential while simultaneously maintaining its physical integrity.

REFERENCES

ABARENKOV, K. et al. The UNITE database for molecular identification and taxonomic communication of fungi and other eukaryotes: sequences, taxa and classifications reconsidered. *Nucleic Acids Research*, v. 52, p. D791–D797, 2024. https://doi.org/10.1093/nar/gkad1039

ALVARES, C. A. et al. Köppen's climate classification map for Brazil. *Meteorologische Zeitschrift*, v. 22, p. 711–728, 2013. https://doi.org/10.1127/0941-2948/2013/0507

ATANGANA, A. et al. Definitions and Classification of Agroforestry Systems. In: _____. *Tropical Agroforestry*. Dordrecht: Springer Netherlands, 2014. p. 35–47. https://doi.org/10.1007/978-94-007-7723-1_3

AYRES, E. et al. Tree species traits influence soil physical, chemical, and biological properties in high elevation forests. *PLoS One*, v. 4, 2009. https://doi.org/10.1371/journal.pone.0005964

BANNING, N. C. et al. Soil microbial community successional patterns during forest ecosystem restoration. *Applied and Environmental Microbiology*, v. 77, p. 6158–6164, 2011. https://doi.org/10.1128/AEM.00764-11

BATISTELLA, M. et al. Agroforestry in Tomé-Açu: An Alternative to Pasture in the Amazon. In: BRONDÍZIO, E. S.; MORAN, E. F. (Eds.). *Human-Environment Interactions*. Dordrecht: Springer Netherlands, 2013. p. 321–342. https://doi.org/10.1007/978-94-007-4780-7_14

BATTISTUZZI, F. U.; HEDGES, S. B. A major clade of prokaryotes with ancient adaptations to life on land. *Molecular Biology and Evolution*, v. 26, p. 335–343, 2009. https://doi.org/10.1093/molbev/msn247

BENK, S. A. et al. Fueling Diversity in the Subsurface: Composition and Age of Dissolved Organic Matter in the Critical Zone. *Frontiers in Earth Science*, v. 7, 2019. https://doi.org/10.3389/feart.2019.00296

BERNI, J. A. J. et al. Thermal and narrowband multispectral remote sensing for vegetation monitoring from an unmanned aerial vehicle. *IEEE Transactions on Geoscience and Remote Sensing*, v. 47, p. 722–738, 2009. https://doi.org/10.1109/TGRS.2008.2010457

BIELUCZYK, W. et al. Restoration of soil health by Amazonian secondary forests is severely eroded by slash-and-burn recurrence. *Catena* v. 254, 2025. https://doi.org/10.1016/j.catena.-2025.108925

BIELUCZYK, W. et al. Slash-and-burn agriculture disrupts the carbon storage potential and ecosystem multifunctionality of Amazon's secondary forests. *Agriculture, Ecosystems & Environment*, v. 381, 2025. https://doi.org/10.1016/j.agee.2024.109413

BIELUCZYK, W. et al. Forest restoration rehabilitates soil multifunctionality in riparian zones of sugarcane production landscapes. *Science of The Total Environment*, v. 888, 2023. https://doi.org/10.1016/j.scitotenv.2023.164175

BROADBENT, E. N. et al. Integrating stand and soil properties to understand foliar nutrient dynamics during forest succession following slash-and-burn agriculture in the Bolivian Amazon. *PLoS One*, v. 9, 2014. https://doi.org/10.1371/journal.pone.0086042

BRODY, J. R.; KERN, S. E. History and principles of conductive media for standard DNA electrophoresis. *Analytical Biochemistry*, 2004. https://doi.org/10.1016/j.ab.2004.05.054

BUCKERIDGE, K. M. et al. Environmental and microbial controls on microbial necromass recycling, an important precursor for soil carbon stabilization. *Communications Earth & Environment*, v. 1, 2020. https://doi.org/10.1038/s43247-020-00031-4

BÜNEMANN, E. K. et al. Soil quality – A critical review. *Soil Biology and Biochemistry*, 2018. https://doi.org/10.1016/j.soilbio.2018.01.030

CALLAHAN, B. J. et al. DADA2: High-resolution sample inference from Illumina amplicon data. *Nature Methods*, v. 13, p. 581–583, 2016. https://doi.org/10.1038/nmeth.3869

CAMPS-VALLS, G. et al. A unified vegetation index for quantifying the terrestrial biosphere. *Science Advances*, v. 7, n. 9, eabc7447, 2021.

CAPORASO, J. G. et al. Global patterns of 16S rRNA diversity at a depth of millions of sequences per sample. *Proceedings of the National Academy of Sciences*, v. 108, p. 4516–4522, 2011. https://doi.org/10.1073/pnas.1000080107

CARDOZO, E. G. et al. Agroforestry systems recover tree carbon stock faster than natural succession in Eastern Amazon, Brazil. *Agroforestry Systems*, v. 96, p. 941–956, 2022. https://doi.org/10.1007/s10457-022-00754-7

CARNEIRO, R. G. et al. A soil health assessment tool for vegetable cropping systems in tropical soils based on beta-glucosidase, arylsulfatase, and soil organic carbon. *Applied Soil Ecology*, v. 198, 2024. https://doi.org/10.1016/j.apsoil.2024.105394

CELENTANO, D. et al. Carbon sequestration and nutrient cycling in agroforestry systems on degraded soils of Eastern Amazon, Brazil. *Agroforestry Systems*, v. 94, p. 1781–1792, 2020. https://doi.org/10.1007/s10457-020-00496-4

CEZAR, R. M. et al. Soil biological properties in multistrata successional agroforestry systems and in natural regeneration. *Agroforestry Systems*, v. 89, p. 1035–1047, 2015. https://doi.org/10.1007/s10457-015-9833-7

CHANTIGNY, M. H. Dissolved and water-extractable organic matter in soils: A review on the influence of land use and management practices. *Geoderma*, v. 113, p. 357–380, 2003. https://doi.org/10.1016/S0016-7061(02)00370-1

CHAOPRICHA, N. T.; MARÍN-SPIOTTA, E. Soil burial contributes to deep soil organic carbon storage. *Soil Biology and Biochemistry*, 2014. https://doi.org/10.1016/j.soilbio.2013.11.011

CHERUBIN, M. R. et al. Soil quality indexing strategies for evaluating sugarcane expansion in Brazil. PLoS One. v 11, p 1–26, 2016a. https://doi.org/10.1371/journal.pone.0150860.

CHERUBIN, M. R. et al. A Soil Management Assessment Framework (SMAF) Evaluation of Brazilian Sugarcane Expansion on Soil Quality. *Soil Science Society of America Journal*, v. 80, p. 215–226, 2016b. https://doi.org/10.2136/sssaj2015.09.0328

CHERUBIN, M. R. et al. Soil health response to sugarcane straw removal in Brazil. *Industrial Crops and Products*, v. 163, 2021. https://doi.org/10.1016/j.indcrop.2021.113315

CONDIT, R. et al. Beta-Diversity in Tropical Forest Trees. *Science*, v. 295, p. 666–669, 2002. https://doi.org/10.1126/science.1066854

COTRUFO, M. F.; LAVALLEE, J. M. Soil organic matter formation, persistence, and functioning: A synthesis of current understanding to inform its conservation and regeneration. In: *Advances in Agronomy*. Hoboken: Academic Press, 2022. p. 1–66. https://doi.org/10.1016/bs.agron.2021.11.002

COTRUFO, M. F. et al. Soil carbon storage informed by particulate and mineral-associated organic matter. *Nature Geoscience*, v. 12, p. 989–994, 2019. https://doi.org/10.1038/s41561-019-0484-6

COTRUFO, M. F. et al. Formation of soil organic matter via biochemical and physical pathways of litter mass loss. *Nature Geoscience*, v. 8, p. 776–779, 2015. https://doi.org/10.1038/ngeo2520

CUTLER, N. A. et al. Long-term changes in soil microbial communities during primary succession. *Soil Biology and Biochemistry*, v. 69, p. 359–370, 2014. https://doi.org/10.1016/j.soilbio.2013.11.022

DA VEIGA LEPREVOST, F. et al. BioContainers: An open-source and community-driven framework for software standardization. *Bioinformatics*, v. 33, p. 2580–2582, 2017. https://doi.org/10.1093/bioinformatics/btx192

DAVIDSON, E. A. et al. The Amazon basin in transition. *Nature*, 2012. https://doi.org/10.1038/nature10717

DAVIDSON, E. A. et al. Nitrogen and phosphorus limitation of biomass growth in a tropical secondary forest. *Ecological Applications*, v. 14, 2004. https://doi.org/10.1890/01-6006

DE OLIVEIRA, H. M. R. et al. Repercussion of pastoral systems in C and N fractions stock in northeast Amazonia. *Catena*, v. 208, 2022. https://doi.org/10.1016/j.catena.2021.105742

D'OLIVEIRA, M. V. N. et al. Forest natural regeneration and biomass production after slash and burn in a seasonally dry forest in the Southern Brazilian Amazon. *Forest Ecology and Management*, v. 261, p. 1490–1498, 2011. https://doi.org/10.1016/j.foreco.2011.01.014

EL HILALI, R. et al. Cultivation, identification, and application of arbuscular mycorrhizal fungi associated with date palm plants in Drâa-Tafilalet oasis. *Rhizosphere*, v. 22, 2022. https://doi.org/10.1016/j.rhisph.2022.100521

ELEVITCH, C. R. et al. Agroforestry standards for regenerative agriculture. *Sustainability*, v. 10, 2018. https://doi.org/10.3390/su10093337

ENGLAND, L. S. et al. Extraction, detection and persistence of extracellular DNA in forest litter microcosms. *Molecular and Cellular Probes*, v. 18, p. 313–319, 2004. https://doi.org/10.1016/j.mcp.2004.05.001

EWELS, P. et al. MultiQC: summarize analysis results for multiple tools and samples in a single report. *Bioinformatics*, v. 32, p. 3047–3048, 2016. https://doi.org/10.1093/bioinformatics/btw354

EWELS, P. et al. The nf-core framework for community-curated bioinformatics pipelines. *Nature Biotechnology*, v. 38, p. 276–278, 2020. https://doi.org/10.1038/s41587-020-0439-x

FLORES, B. M. et al. Editorial special issue: plant-soil interactions in the Amazon rainforest. *Plant and Soil*, v. 450, p. 1–9, 2020. https://doi.org/10.1007/s11104-020-04544-x

GMACH, M. R. et al. Processes that influence dissolved organic matter in the soil: A review. *Scientia Agricola*, 2020. https://doi.org/10.1590/1678-992x-2018-0164

GRÜNING, B. et al. Bioconda: sustainable and comprehensive software distribution for the life sciences. *Nature Methods*, v. 15, p. 475–476, 2018. https://doi.org/10.1038/s41592-018-0046-7

HABOUDANE, D. et al. Hyperspectral vegetation indices and novel algorithms for predicting green LAI of crop canopies: Modeling and validation in the context of precision agriculture. *Remote Sensing of Environment*, v. 90, p. 337–352, 2004. https://doi.org/10.1016/j.rse.2003.12.013

HABOUDANE, D. et al. Remote estimation of crop chlorophyll content using spectral indices derived from hyperspectral data. *IEEE Transactions on Geoscience and Remote Sensing*, p. 423–436, 2008. https://doi.org/10.1109/TGRS.2007.904836

HERRERA, R. et al. Amazon ecosystems: Their structure and functioning with particular emphasis on nutrients. *Interciencia*, v. 3, p. 223–232, 1978.

ISAAC, M. E.; BORDEN, K. A. Nutrient acquisition strategies in agroforestry systems. *Plant and Soil*, 2019. https://doi.org/10.1007/s11104-019-04232-5

JENKINS, C. N. et al. Global patterns of terrestrial vertebrate diversity and conservation. *Proceedings of the National Academy of Sciences*, v. 110, p. E2603–E2610, 2013. https://doi.org/10.1073/pnas.1302251110

JONES, D. L.; WILLETT, V. B. Experimental evaluation of methods to quantify dissolved organic nitrogen (DON) and dissolved organic carbon (DOC) in soil. *Soil Biology and Biochemistry*, v. 38, p. 991–999, 2005. https://doi.org/10.1016/j.soilbio.2005.08.012

JORDAN, C. F.; HERRERA, R. Tropical Rain Forests: Are Nutrients Really Critical? *The American Naturalist*, v. 117, p. 167–180, 1981. https://doi.org/10.1086/283696

JOSE, S. Agroforestry for ecosystem services and environmental benefits: An overview. *Agroforestry Systems*, 2009. https://doi.org/10.1007/s10457-009-9229-7

KAISER, K.; KALBITZ, K. Cycling downwards - dissolved organic matter in soils. *Soil Biology and Biochemistry*, v. 52, p. 29–32, 2012. https://doi.org/10.1016/j.soilbio.2012.04.002

KALLENBACH, C. M. et al. Direct evidence for microbial-derived soil organic matter formation and its ecophysiological controls. *Nature Communications*, v. 7, 2016. https://doi.org/10.1038/ncomms13630

KOCH, H. et al. Complete nitrification: insights into the ecophysiology of comammox Nitrospira. *Applied Microbiology and Biotechnology*, 2019. https://doi.org/10.1007/s00253-018-9486-3

LACERDA-JÚNIOR, G. V. et al. Land use and seasonal effects on the soil microbiome of a Brazilian dry forest. *Frontiers in Microbiology*, v. 10, 2019. https://doi.org/10.3389/fmicb.2019.00648

LAHTI, L. et al. Microbiome r package. *Tools Microbiome Anal R*, 2017.

LANGE, M. et al. Plant diversity increases soil microbial activity and soil carbon storage. *Nature Communications*, v. 6, 2015. https://doi.org/10.1038/ncomms7707

LAURANCE, W. F. et al. Relationship between soils and Amazon forest biomass: A landscape-scale study. *Forest Ecology and Management*, v. 118, p. 127–138, 1999. https://doi.org/10.1016/S0378-1127(98)00494-0

LE MAIRE, G. et al. Calibration and validation of hyperspectral indices for the estimation of broadleaved forest leaf chlorophyll content, leaf mass per area, leaf area index and leaf canopy biomass. *Remote Sensing of Environment*, v. 112, p. 3846–3864, 2008. https://doi.org/10.1016/j.rse.2008.06.005

LEHTOVIRTA-MORLEY, L. E. et al. Nitrosotalea devaniterrae gen. nov., sp. nov. and Nitrosotalea sinensis sp. nov., two acidophilic ammonia oxidising archaea isolated from acidic soil, and proposal of the new order Nitrosotaleales ord. nov. within the class Nitrososphaeria of the phylum Nitrososphaerota. *International Journal of Systematic and Evolutionary Microbiology*, v. 74, 2024. https://doi.org/10.1099/ijsem.0.006387

LEITE, M. F. A. et al. Microbiome resilience of Amazonian forests: Agroforest divergence to bacteria and secondary forest succession convergence to fungi. *Global Change Biology*, v. 29, p. 1314–1327, 2023. https://doi.org/10.1111/gcb.16556

LEUTHOLD, S. J. et al. Physical fractionation techniques. In: *Encyclopedia of Soils in the Environment*. Elsevier, 2023. p. V2-68-V2-80. https://doi.org/10.1016/B978-0-12-822974-3.00067-7

LIANG, Y. et al. Long-term forest restoration influences succession patterns of soil bacterial communities. *Environmental Science and Pollution Research*, v. 28, p. 20598–20607, 2021. https://doi.org/10.1007/s11356-020-11849-y

LOPES, A. A. de C. et al. Interpretation of Microbial Soil Indicators as a Function of Crop Yield and Organic Carbon. *Soil Science Society of America Journal*, v. 77, p. 461–472, 2013. https://doi.org/10.2136/sssaj2012.0191

LOPES, A. A. de C. et al. Temporal variation and critical limits of microbial indicators in oxisols in the Cerrado, Brazil. *Geoderma Regional*, v. 12, p. 72–82, 2018. https://doi.org/10.1016/j.geodrs.2018.01.003

LORENZ, K.; LAL, R. Agroforestry Systems. In: _____. *Carbon Sequestration in Agricultural Ecosystems*. Cham: Springer International Publishing, 2018. p. 235–260. https://doi.org/10.1007/978-3-319-92318-5_6

LORENZ, K.; LAL, R. The Depth Distribution of Soil Organic Carbon in Relation to Land Use and Management and the Potential of Carbon Sequestration in Subsoil Horizons. *Advances in Agronomy*, 2005. https://doi.org/10.1016/S0065-2113(05)88002-2

LUCHETA, A. R. et al. Fungal Community Assembly in the Amazonian Dark Earth. *Microbial Ecology*, v. 71, p. 962–973, 2016. https://doi.org/10.1007/s00248-015-0703-7

LUGLI, L. F. et al. Rapid responses of root traits and productivity to phosphorus and cation additions in a tropical lowland forest in Amazonia. *New Phytologist*, v. 230, p. 116–128, 2021. https://doi.org/10.1111/nph.17154

MALAVOLTA, E. et al. *Evaluation of the nutritional state of plants: principles and applications*. Piracicaba: Associação Brasileira para Pesquisa da Potassa e do Fosfato, 1989.

MARKEWITZ, D. et al. Nutrient loss and redistribution after forest clearing on a highly weathered soil in Amazonia. *Ecological Applications*, v. 14, 2004. https://doi.org/10.1890/01-6016

MARQUARDT, K. et al. Forest Dynamics in the Peruvian Amazon: Understanding Processes of Change. *Small-scale Forestry*, v. 18, p. 81–104, 2019. https://doi.org/10.1007/s11842-018-9408-3

MARTIN, M. Cutadapt removes adapter sequences from high-throughput sequencing reads. *EMBnet Journal*, v. 17, p. 10, 2011. https://doi.org/10.14806/ej.17.1.200

MARTINELLI, L. A. et al. *Desvendando questões ambientais com isótopos estáveis*. São Paulo: Oficina de Textos, 2009.

MARTIUS, C. et al. Litter fall, litter stocks and decomposition rates in rainforest and agroforestry sites in central Amazonia. *Nutrient Cycling in Agroecosystems*, v. 68, p. 137–154, 2004. https://doi.org/10.1023/B:FRES.0000017468.76807.50

MCMURDIE, P. J.; HOLMES, S. Phyloseq: An R Package for Reproducible Interactive Analysis and Graphics of Microbiome Census Data. *PLoS One*, v. 8, 2013. https://doi.org/10.1371/journal.pone.0061217

MENDES, L. W. et al. Land-use system shapes soil bacterial communities in Southeastern Amazon region. *Applied Soil Ecology*, v. 95, p. 151–160, 2015a. https://doi.org/10.1016/j.apsoil.2015.06.005

MENDES, L. W. et al. Soil-Borne Microbiome: Linking Diversity to Function. *Microbial Ecology*, v. 70, p. 255–265, 2015b. https://doi.org/10.1007/s00248-014-0559-2

MILORI, D. M. B. P. et al. Organic Matter Study of Whole Soil Samples Using Laser-Induced Fluorescence Spectroscopy. *Soil Science Society of America Journal*, v. 70, p. 57–63, 2006. https://doi.org/10.2136/sssaj2004.0270

MILORI, D. M. B. P. et al. Humification degree of soil humic acids determined by fluorescence spectroscopy. *Soil Science*, v. 167, p. 739–749, 2002. https://doi.org/10.1097/00010694-200211000-00004

MITCHELL, E. et al. Important constraints on soil organic carbon formation efficiency in subtropical and tropical grasslands. *Global Change Biology*, v. 27, p. 5383–5391, 2021. https://doi.org/10.1111/gcb.15807

MOHRI, H. et al. Assessment of ecosystem services in homegarden systems in Indonesia, Sri Lanka, and Vietnam. *Ecosystem Services*, v. 5, p. 124–136, 2013. https://doi.org/10.1016/j.ecoser.2013.07.006

MUELLER, R. C. et al. Land use change in the Amazon rain forest favours generalist fungi. *Functional Ecology*, v. 30, p. 1845–1853, 2016. https://doi.org/10.1111/1365-2435.12651

MÜLLER, M. M. L. et al. The relationship between pasture degradation and soil properties in the Brazilian amazon: A case study. *Agriculture, Ecosystems & Environment*, v. 103, p. 279–288, 2004. https://doi.org/10.1016/j.agee.2003.12.003

MYNENI, R. B. et al. The Interpretation of Spectral Vegetation Indexes. *IEEE Transactions on Geoscience and Remote Sensing*, v. 33,n. 2, p. 481-486, 1995.

NAIR, P. K. R. Grand challenges in agroecology and land use systems. *Frontiers in Environmental Science*, v. 2, 2014. https://doi.org/10.3389/fenvs.2014.00001

NAIR, P. K. R. Agroforestry: Trees in Support of Sustainable Agriculture. In: *Reference Module in Earth Systems and Environmental Sciences*. Elsevier, 2013. https://doi.org/10.1016/B978-0-12-409548-9.05088-0

NAIR, P. K. R. et al. Carbon Sequestration in Agroforestry Systems. *Advances in Agronomy*, p. 237–307, 2010. https://doi.org/10.1016/S0065-2113(10)08005-3

NAVAL, M. L. M. et al. Impacts of repeated forest fires and agriculture on soil organic matter and health in southern Amazonia. *Catena*, v. 254, 2025. https://doi.org/10.1016/j.catena.2025.108924

NAVARRETE, A. A. et al. Acidobacterial community responses to agricultural management of soybean in Amazon forest soils. *FEMS Microbiology Ecology*, v. 83, p. 607–621, 2013. https://doi.org/10.1111/1574-6941.12018

NAVARRETE, A. A. et al. Soil microbiome responses to the short-term effects of Amazonian deforestation. *Molecular Ecology*, v. 24, p. 2433–2448, 2015. https://doi.org/10.1111/mec.13172

NUNES, C. A. et al. Linking land-use and land-cover transitions to their ecological impact in the Amazon. *Proceedings of the National Academy of Sciences*, v. 119, 2022. https://doi.org/10.1073/pnas.2202310119

OKSANEN, A. J. et al. Package 'vegan'. Vienna: R System, 2020.

PACHECO, N. A.; BASTOS, T. X. *Caracterização climática do município de Tomé-Açu, PA*. Belém, PA: Embrapa Amazônia Oriental, 2001.

PEDRINHO, A. et al. Impacts of deforestation and forest regeneration on soil bacterial communities associated with phosphorus transformation processes in the Brazilian Amazon region. *Ecological Indicators*, v. 146, 2023. https://doi.org/10.1016/j.ecolind.2022.109779

PHILIPPOT, L. et al. Microbial Community Resilience across Ecosystems and Multiple Disturbances. *Microbiology and Molecular Biology Reviews*, v. 85, 2021. https://doi.org/10.1128/mmbr.00026-20

PINHO, R. C. et al. Agroforestry and the Improvement of Soil Fertility: A View from Amazonia. *Applied and Environmental Soil Science*, v. 2012, p. 1–11, 2012. https://doi.org/10.1155/2012/616383

POWERS, J. S.; MARÍN-SPIOTTA, E. Ecosystem Processes and Biogeochemical Cycles in Secondary Tropical Forest Succession. *Annual Review of Ecology, Evolution, and Systematics*, v. 48, p. 497–519, 2017. https://doi.org/10.1146/annurev-ecolsys-110316

QUAST, C. et al. The SILVA ribosomal RNA gene database project: improved data processing and web-based tools. *Nucleic Acids Research*, v. 41, p. D590–D596, 2012. https://doi.org/10.1093/nar/gks1219

RIGGS, C. E. et al. Nitrogen addition changes grassland soil organic matter decomposition. *Biogeochemistry*, v. 125, p. 203–219, 2015. https://doi.org/10.1007/s10533-015-0123-2

RINOT, O. et al. Soil health assessment: A critical review of current methodologies and a proposed new approach. *Science of the Total Environment*, v. 648, p. 1484–1491, 2019. https://doi.org/10.1016/j.scitotenv.2018.08.259

ROCHA, A. V. S. *Microbial necromass, carbon and agriculture: combining living and dead microbes to reveal carbon dynamics under agroforestry in the Amazon*. 2024. Tese (Doutorado) – Escola Superior de Agricultura Luiz de Queiroz, Universidade de São Paulo, Piracicaba. https://doi.org/10.11606/D.11.2024.tde-10092024-152039

RODRIGUES, J. L. M. et al. Conversion of the Amazon rainforest to agriculture results in biotic homogenization of soil bacterial communities. *Proceedings of the National Academy of Sciences of the USA*, v. 110, p. 988–993, 2013. https://doi.org/10.1073/pnas.1220608110

ROTH, V. N. et al. Persistence of dissolved organic matter explained by molecular changes during its passage through soil. *Nature Geoscience*, v. 12, p. 755–761, 2019. https://doi.org/10.1038/s41561-019-0417-4

SAATCHI, S. et al. Distribution of aboveground live biomass in the Amazon basin. *Global Change Biology*, v. 13, p. 816–837, 2007. https://doi.org/10.1111/j.1365-2486.2007.01323.x

SANTOS, C. H. dos et al. Performance Evaluation of a Portable Laser-Induced Fluorescence Spectroscopy System for the Assessment of the Humification Degree of the Soil Organic Matter. *Journal of the Brazilian Chemical Society*, v. 26, p. 775–783, 2015. https://doi.org/10.5935/0103-5053.20150039

SANTOS, H. G. et al. *O novo mapa de solos do Brasil*: legenda atualizada. Rio de Janeiro: Embrapa Solos, 2011. 67 p.

SCHAEFER, C. E. G. R. et al. Soil and vegetation carbon stocks in Brazilian Western Amazonia: Relationships and ecological implications for natural landscapes. *Environmental Monitoring and Assessment*, v. 140, p. 279–289, 2008. https://doi.org/10.1007/s10661-007-9866-0

SEGATA, N. et al. Metagenomic biomarker discovery and explanation. *Genome Biology*, v. 12, 2011. https://doi.org/10.1186/gb-2011-12-6-r60

SENEVIRATNE, G. et al. Nutrient Cycling and Safety-net Mechanism in the Tropical Homegardens. *International Journal of Agricultural Research*, v. 1, p. 169–182, 2006. https://doi.org/10.3923/ijar.2006.169.182

SIMON, C. da P. et al. Soil quality literature in Brazil: A systematic review. *Revista Brasileira de Ciência do Solo*, 2022. https://doi.org/10.36783/18069657rbcs20210103

SLIK, J. W. F. et al. An estimate of the number of tropical tree species. *Proceedings of the National Academy of Sciences of the USA*, v. 112, p. 7472–7477, 2015. https://doi.org/10.1073/pnas.1423147112

SOONG, J. L. et al. Quantification and FTIR characterization of dissolved organic carbon and total dissolved nitrogen leached from litter: a comparison of methods across litter types. *Plant and Soil*, v. 385, p. 125–137, 2014. https://doi.org/10.1007/s11104-014-2232-4

SOONG, J. L. et al. A new conceptual model on the fate and controls of fresh and pyrolized plant litter decomposition. *Biogeochemistry*, v. 124, p. 27–44, 2015. https://doi.org/10.1007/s10533-015-0079-2

SPARKS, D. L. et al. The Chemistry of Soil Acidity. In: *Environmental Soil Chemistry*. Elsevier, 2024. p. 381–410. https://doi.org/10.1016/B978-0-443-14034-1.00009-5

STRAUB, D. et al. Interpretations of Environmental Microbial Community Studies Are Biased by the Selected 16S rRNA (Gene) Amplicon Sequencing Pipeline. *Frontiers in Microbiology*, v. 11, 2020. https://doi.org/10.3389/fmicb.2020.550420

TADINI, A. M. et al. Soil organic matter in podzol horizons of the Amazon region: Humification, recalcitrance, and dating. *Science of the Total Environment*, v. 613–614, p. 160–167, 2018. https://doi.org/10.1016/j.scitotenv.2017.09.068

TADINI, A. M. et al. Evaluation of soil organic matter from integrated production systems using laser-induced fluorescence spectroscopy. *Soil and Tillage Research*, v. 211, 2021. https://doi.org/10.1016/j.still.2021.105001

TEIXEIRA, P. C. et al. *Manual de métodos de análise de solo*. Rio de Janeiro: Embrapa Solos, 2017.

USINOWICZ, J. et al. Temporal coexistence mechanisms contribute to the latitudinal gradient in forest diversity. *Nature*, v. 550, p. 105–108, 2017. https://doi.org/10.1038/nature24038

VAN RAIJ, B. et al. *Análise química para avaliação da fertilidade de solos tropicais*. Campinas: Instituto Agronômico, 2001.

VENTURINI, A. M. et al. Increased soil moisture intensifies the impacts of forest-to-pasture conversion on methane emissions and methane-cycling communities in the Eastern Amazon. *Environmental Research*, v. 212, 2022. https://doi.org/10.1016/j.envres.2022.113139

VILLA, P. M. et al. Intensification of shifting cultivation reduces forest resilience in the northern Amazon. *Forest Ecology and Management*, v. 430, p. 312–320, 2018. https://doi.org/10.1016/j.foreco.2018.08.014

WHITE, T. J. et al. Amplification and direct sequencing of fungal ribosomal RNA genes for phylogenetics. In: INNIS, M.A. et al. (eds.). *PCR Protocols*: A Guide to Methods and Applications. New York: Academic Press, 1990. p. 315-322. https://dx.doi.org/10.1016/B978-0-12-372180-8.50042-1

WICKHAM, H.; CHANG, W. Package 'ggplot2.' *Create elegant data visualisations using the grammar of graphics*, v. 2, p. 1–189, 2016.

XU, R. K. et al. Adsorption Properties of Subtropical and Tropical Variable Charge Soils: Implications from Climate Change and Biochar Amendment. *Advances in Agronomy*, p. 1–58, 2016. https://doi.org/10.1016/bs.agron.2015.09.001

YOUNG, K. J. Mimicking Nature: A Review of Successional Agroforestry Systems as an Analogue to Natural Regeneration of Secondary Forest Stands. p. 179–209, 2017. https://doi.org/10.1007/978-3-319-69371-2_8

ZENG, Y. et al. Optical vegetation indices for monitoring terrestrial ecosystems globally. *Nature Reviews Earth & Environment*, v. 3, p. 477–493, 2022. https://doi.org/10.1038/s

APPENDICES

Appendix A: Supplementary material

Supplementary Figure 1. Soil texture class of the soil samples of the study

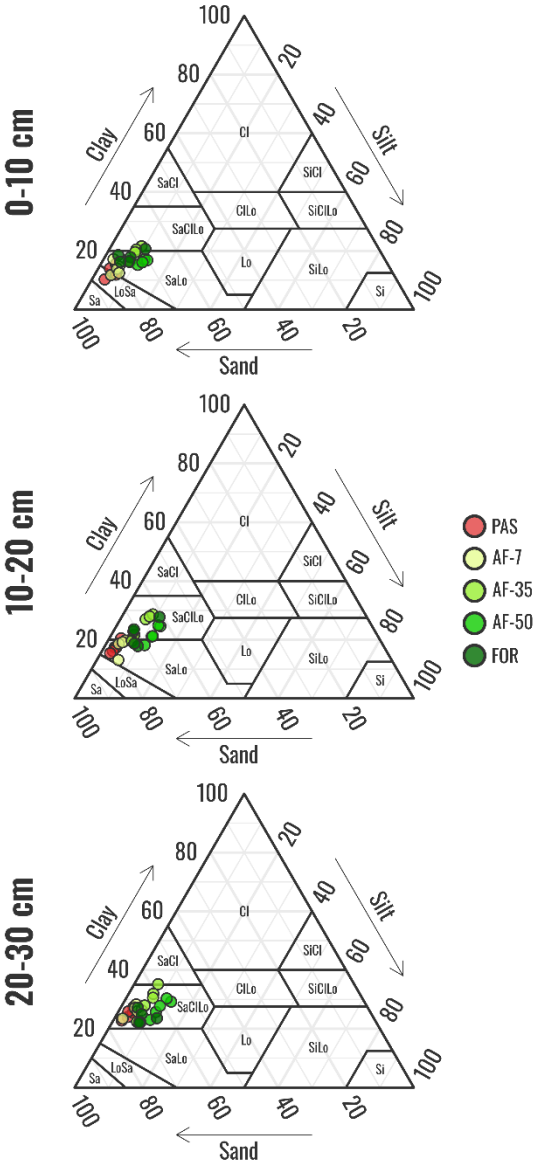

Supplementary Table 1. Description of land use systems studied

Land use	System description	Geolocation
Pasture	Abandoned pasture (PAS)	2°32'49.8" S, 48°21'22.1" W
Agroforest	7 years old Açaí (*Euterpe oleracea* Mart.) and Cocoa (*Theobroma cacao* L.) based agroforest (AF-7)	2°32'42.7" S, 48°21'35.4" W
	35 years old Açaí (*Euterpe oleracea* Mart.) and Cocoa (*Theobroma cacao* L.) agroforest, with mature Taperebá (*Spondias lutea*) and Freijó (*Cordia goeldiana*) trees	2°28'56.6" S, 48°16'42.0" W
	50 years old Açaí (*Euterpe oleracea* Mart.) and Cocoa (*Theobroma cacao* L.) agroforest, with mature Guaraná (*Paullinia cupana*), Palheteira (*Clitoria fairchildiana*), Jacarandá (*Jacaranda copaia*), Morototó (*Schefflera morototoni*) e Manga (*Mangifera indica*) trees	2°24'00.7" S, 48°09'57.2" W
Primary Forest	Primary Amazon Forest	2°35'51.9" S, 48°21'28.6"W

Supplementary Table 2. Description of primers used in qPCR

Gene	Target	Primers	Sequence (5'-3)	Reference
16S rRNA	Bacteria	515f	GTGCCAGCMGCCGCGGTAA	(Caporaso et al., 2011)
		806r	GGACTACHVGGGTWTCTAAT	
ITS *Fungi*	Fungi	ITS1f	TCCGTAGGTGAACCTGCGG	(White et al., 1990)
		ITS2r	GCTGCGTTCTTCATCGATGC	

Supplementary Table 3. Model[a] of the soil functions framework and indicators for developing the soil health index (SHI).

Index	Component	Weight I	Soil functions	Weight II	Indicators	Weight III
SHI	Physical	0.33	Support root growth	0.5	Bulk density	1.0
			Water storage and aeration	0.5	MiP	0.5
					MaP	0.5
	Chemical	0.33	Soil acidity regulation	0.33	pH	1.0
			Nutrient availability	0.33	N	0.2
					P	0.2
					K	0.2
					Ca	0.2
					Mg	0.2
			Nutrient storage	0.33	CEC	1.0
			Energy for microbial activity	0.33	C	1.0
	Biological	0.33	Soil nutrient cycling	0.33	Beta-gluc	0.33
					Aryl	0.33
					Phos	0.33
			Habitat for microorganisms	0.33	Fung-ITS	0.25
					Bac-16S	0.25
					Fung-Div	0.25
					Bac-Div	0.25

[a]Adapted structure from previous outlines (Cherubin et al., 2016a, 2016b; Bünemann et al., 2018; Rinot et al., 2019; Simon et al., 2022). **Bd**: bulk density, **MaP**: macroporosity, **MiP**: microporosity, **pH**: pH_{CaCl2}, **N**: total nitrogen content, **P**: available phosphorus, **K**: available potassium, **CEC**: cation exchange capacity in pH 7.0, **C**: total carbon content, **Beta-gluc**: β-glucosidase activity, **Aryl**: arylsulfatase activity, **Phos**: acid-phosphatase activity, **Fung-ITS**: total fungal community, **bac-16S**: total bacterial community, **Fung-div**: fungal community Shannon-wiener diversity index, **Bac-Div**: bacterial community Shannon-wiener diversity index

Supplementary Table 4. Soil LEFse from 0-10 cm soil bacteria

Site	Taxa	LDA	p-value
PAS	p__Firmicutes — g__Bacillus	4.726	0.0002
	p__Actinobacteriota — g__Conexibacter	4.144	0.0003
	p__Myxococcota — g__Haliangium	3.943	0.0011
	p__Firmicutes — g__Lysinibacillus	3.692	0.0020
	p__Myxococcota — g__Anaeromyxobacter	3.487	0.0036
AF-7	p__Proteobacteria — g__Pedomicrobium	4.200	0.0001
	p__Firmicutes — g__Tumebacillus	3.749	0.0003
	p__Proteobacteria — g__mle1-7	3.557	0.0003
	p__Proteobacteria — g__Nordella	3.498	0.0004
	p__Actinobacteriota — g__Luedemannella	3.480	0.0004
AF-35	p__Actinobacteriota — g__Gaiella	4.114	0.0002
	p__Nitrospirota — g__Nitrospira	3.802	0.0001
	p__Proteobacteria — g__Hyphomicrobium	3.760	0.0003
	p__Proteobacteria — g__MND1	3.461	0.0024
	p__Bacteroidota — g__Flavobacterium	3.339	0.0008
AF-50	p__Proteobacteria — g__Pseudolabrys	4.358	0.0001
	p__Verrucomicrobiota — g__Candidatus Udaeobacter	4.120	0.0140
	p__Verrucomicrobiota — g__ADurb.Bin063-1	3.635	0.0030
	p__Proteobacteria — g__Roseiarcus	3.576	0.0007
	p__Firmicutes — g__Anaerocolumna	3.464	0.0126
FOR	p__Proteobacteria — g__Acidibacter	4.341	0.0002
	p__Acidobacteriota — g__Candidatus Koribacter	4.312	0.0005
	p__Actinobacteriota — g__Acidothermus	4.270	0.0009
	p__Proteobacteria — g__Bradyrhizobium	4.228	0.0003
	p__Verrucomicrobiota — g__Candidatus Xiphinematobacter	4.065	0.0020

Supplementary Table 5. Soil LEFse from 0-10 cm soil fungi

Site	Taxa	LDA	p-value
PAS	p__Ascomycota — g__Sodiomyces	4.591	0.0003
	p__Ascomycota — g__Penicillium	4.449	0.0036
	p__Ascomycota — g__Aspergillus	4.252	0.0015
	p__Ascomycota — g__Westerdykella	4.220	0.0002
	p__Basidiomycota — g__Clitocybe	4.110	0.0001
AF-7	p__Ascomycota — g__Fusarium	4.301	0.0044
	p__Ascomycota — g__Stromatoneurospora	4.223	0.0051
	p__Ascomycota — g__Amorocoelophoma	4.156	0.0012
	p__Basidiomycota — g__Psathyrella	4.114	0.0003
	p__Ascomycota — g__Rasamsonia	3.850	0.0130
AF-35	p__Mortierellomycota — g__Mortierella	4.354	0.0018
	p__Ascomycota — g__Wallrothiella	4.123	0.0004
	p__Ascomycota — g__Auxarthron	4.080	0.0003
	p__Glomeromycota — g__Pervetustus	4.033	0.0004
	p__Ascomycota — g__Arachnotheca	4.030	0.0004
AF-50	p__Ascomycota — g__Trichoderma	4.502	0.0117
	p__Ascomycota — g__Clonostachys	4.396	0.0010
	p__Ascomycota — g__Chloridium	4.294	0.0080
	p__Ascomycota — g__Talaromyces	4.225	0.0079
	p__Ascomycota — g__Chaetosphaeria	4.000	0.0009
FOR	p__Basidiomycota — g__Hygrocybe	4.038	0.0086
	p__Basidiomycota — g__Entoloma	3.713	0.0160
	p__Ascomycota — g__Scedosporium	3.688	0.0345
	p__Basidiomycota — g__Clitopilus	3.568	0.0003
	p__Ascomycota — g__Melanconiella	3.511	0.0149

Supplementary Table 6. Soil LEFse from 10-20 cm soil bacteria

Site	Taxa	LDA	p-value
PAS	p__Firmicutes — g__Bacillus	4.421	0.0030
	p__Actinobacteriota — g__Conexibacter	4.326	0.0001
	p__Myxococcota — g__Haliangium	3.683	0.0228
	p__Myxococcota — g__Anaeromyxobacter	3.535	0.0003
	p__Firmicutes — g__Tumebacillus	3.499	0.0007
AF-7	p__Proteobacteria — g__Ellin6067	3.258	0.0029
	p__Crenarchaeota — g__Candidatus Nitrosotalea	3.195	0.0100
	p__Firmicutes — g__Pullulanibacillus	3.186	0.0003
	p__Firmicutes — g__Ammoniphilus	3.184	0.0025
	p__Desulfobacterota — g__Geobacter	3.157	0.0024
AF-35	p__Actinobacteriota — g__Gaiella	4.317	0.0005
	p__Verrucomicrobiota — g__Candidatus Udaeobacter	4.227	0.0030
	p__Nitrospirota — g__Nitrospira	3.805	0.0001
	p__Proteobacteria — g__Hyphomicrobium	3.496	0.0021
	p__Gemmatimonadota — g__Gemmatimonas	3.473	0.0003
AF-50	p__Proteobacteria — g__Pseudolabrys	4.271	0.0001
	p__Proteobacteria — g__Pedomicrobium	3.618	0.0014
	p__Firmicutes — g__Alicyclobacillus	3.392	0.0081
	p__Verrucomicrobiota — g__Ellin516	3.379	0.0023
	p__Proteobacteria — g__GOUTA6	3.204	0.0001
FOR	p__Proteobacteria — g__Acidibacter	4.369	0.0002
	p__Actinobacteriota — g__Acidothermus	4.285	0.0005
	p__Acidobacteriota — g__Candidatus Koribacter	4.126	0.0012
	p__Proteobacteria — g__Bradyrhizobium	4.112	0.0003
	p__Verrucomicrobiota — g__Candidatus Xiphinematobacter	4.063	0.0003

Supplementary Table 7. Soil LEFse from 10-20 cm soil fungi

Site	Taxa	LDA	p-value
PAS	p__Ascomycota — g__Sodiomyces	4.097	0.012
	p__Ascomycota — g__Cladosporium	3.996	0.048
	p__Ascomycota — g__Neoidriella	3.638	0.043
	p__Ascomycota — g__Memnoniella	3.562	0.011
	p__Ascomycota — g__Bipolaris	3.433	0.004
AF-7	p__Ascomycota — g__Talaromyces	4.362	0.020
	p__Ascomycota — g__Scedosporium	4.326	0.008
	p__Ascomycota — g__Aspergillus	4.249	0.002
	p__Ascomycota — g__Eleutherascus	4.212	0.038
	p__Ascomycota — g__Fusarium	4.032	0.041
AF-35	p__Ascomycota — g__Humicola	4.386	0.001
	p__Ascomycota — g__Paracremonium	4.219	0.008
	p__Mortierellomycota — g__Mortierella	4.211	0.018
	p__Ascomycota — g__Hansfordia	3.765	0.004
	p__Glomeromycota — g__Pervetustus	3.659	0.043
AF-50	p__Ascomycota — g__Trichoderma	4.540	0.002
	p__Ascomycota — g__Chloridium	4.225	0.010
	p__Ascomycota — g__Auxarthron	4.222	0.0004
	p__Ascomycota — g__Chaetosphaeria	4.189	0.0009
	p__Ascomycota — g__Melanconiella	3.876	0.030
FOR	p__Basidiomycota — g__Hygrocybe	3.792	0.028
	p__Basidiomycota — g__Peniophorella	3.592	0.024
	p__Basidiomycota — g__Dacryopinax	3.569	0.0003
	p__Ascomycota — g__Keithomyces	3.552	0.0002
	p__Basidiomycota — g__Clitopilus	3.509	0.001

Supplementary Table 8. Soil LEFse from 20-30 cm soil bacteria

Site	Taxa	LDA	p-value
PAS	p__Actinobacteriota — g__Corynebacterium	3.720	0.0010
	p__Firmicutes — g__Staphylococcus	3.690	0.0020
	p__Proteobacteria — g__Cronobacter	3.289	0.0020
	p__Proteobacteria — g__Serratia	3.121	0.0370
	p__Firmicutes — g__Leuconostoc	2.915	0.0110
AF-7	p__Bacteroidota — g__Mucilaginibacter	5.501	0.0005
	p__Proteobacteria — g__Methylobacterium	4.158	0.0006
	p__Firmicutes — g__Anoxybacillus	3.586	0.0415
	p__Actinobacteriota — g__Micrococcus	3.028	0.0020
	p__Proteobacteria — g__Haemophilus	2.941	0.0005
AF-35	p__Proteobacteria — g__Acinetobacter	4.844	0.0003
	p__Firmicutes — g__Bacillus	4.482	0.0183
	p__Proteobacteria — g__Pseudomonas	4.280	0.0002
	p__Proteobacteria — g__Sphingomonas	3.956	0.0023
	p__Actinobacteriota — g__Nocardioides	3.782	0.0030
AF-50	p__Verrucomicrobiota — g__Candidatus Udaeobacter	4.148	0.0246
	p__Proteobacteria — g__Pseudolabrys	4.081	0.0025
	p__Actinobacteriota — g__Streptomyces	3.876	0.0011
	p__Proteobacteria — g__Pedomicrobium	3.769	0.0038
	p__Firmicutes — g__Alicyclobacillus	3.679	0.0432
FOR	p__Proteobacteria — g__Acidibacter	4.390	0.0010
	p__Actinobacteriota — g__Acidothermus	4.303	0.0041
	p__Acidobacteriota — g__Candidatus Koribacter	4.221	0.0010
	p__Proteobacteria — g__Bradyrhizobium	4.185	0.0004
	p__Actinobacteriota — g__Conexibacter	4.059	0.0019

Supplementary Table 9. Soil LEFse from 20-30 cm soil fungi

Site	Taxa	LDA	p-value
PAS	p__Ascomycota — g__Cladosporium	4.939507	0.0031
	p__Ascomycota — g__Toxicocladosporium	4.210733	0.0067
	p__Basidiomycota — g__Pisolithus	3.932258	0.0058
	p__Basidiomycota — g__Coriolopsis	3.917037	0.0230
AF-7	p__Ascomycota — g__Paracamarosporium	4.787124	0.0350
	p__Basidiomycota — g__Schizophyllum	4.596222	0.0092
	p__Basidiomycota — g__Malassezia	4.395985	0.0059
	p__Basidiomycota — g__Psathyrella	4.067388	0.0164
	p__Basidiomycota — g__Peniophora	3.911639	0.0032
AF-35	p__Ascomycota — g__Phomatospora	4.43859	0.0363
	p__Ascomycota — g__Epicoccum	3.799854	0.0444
	p__Ascomycota — g__Halosarpheia	3.757943	0.0111
	p__Basidiomycota — g__Marasmius	3.584875	0.0346
	p__Ascomycota — g__Pestalotiopsis	3.376514	0.0166
AF-50	p__Basidiomycota — g__Geastrum	4.543814	0.0143
	p__Basidiomycota — g__Grammothele	4.362712	0.0052
	p__Ascomycota — g__Talaromyces	4.160787	0.0477
	p__Ascomycota — g__Auxarthron	3.964698	0.0074
	p__Ascomycota — g__Trichoderma	3.933814	0.0042
FOR	p__Basidiomycota — g__Dermoloma	4.896856	0.0001
	p__Ascomycota — g__Scedosporium	3.829943	0.0023
	p__Ascomycota — g__Humicola	3.493285	0.0017
	p__Ascomycota — g__Scytalidium	3.445588	0.0249
	p__Basidiomycota — g__Hygroaster	3.375987	0.0350